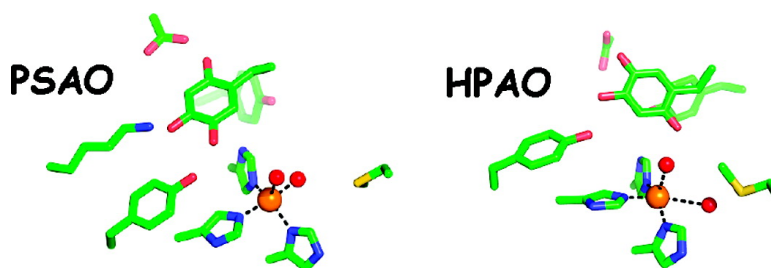# Article

Inner-Sphere Mechanism for Molecular Oxygen Reduction Catalyzed by Copper Amine Oxidases

Arnab Mukherjee, Valeriy V. Smirnov, Michael P. Lanci, Doreen E. Brown, Eric M. Shepard, David M. Dooley, and Justine P. Roth

More About This Article

Additional resources and features associated with this article are available within the HTML version:

- Supporting Information
- Access to high resolution figures
- Links to articles and content related to this article
- Copyright permission to reproduce figures and/or text from this article

View the Full Text HTML

Inner-Sphere Mechanism for Molecular Oxygen Reduction Catalyzed by Copper Amine Oxidases

Arnab Mukherjee,[†] Valeriy V. Smirnov,[†] Michael P. Lanci,[†] Doreen E. Brown,[‡]
Eric M. Shepard,[‡] David M. Dooley,[‡] and Justine P. Roth*,[†]

Department of Chemistry, Johns Hopkins University, 3400 North Charles St., Baltimore, Maryland 21218 and Department of Chemistry and Biochemistry, Montana State University, Bozeman, Montana 59717

Received February 24, 2008; E-mail: jproth@jhu.edu

Abstract: Copper and topaquinone (TPQ) containing amine oxidases utilize O_2 for the metabolism of biogenic amines while concomitantly generating H_2O_2 for use by the cell. The mechanism of O_2 reduction has been the subject of long-standing debate due to the obscuring influence of a proton-coupled electron transfer between the tyrosine-derived TPQ and copper, a rapidly established equilibrium precluding assignment of the enzyme in its reactive form. Here, we show that substrate-reduced pea seedling amine oxidase (PSAO) exists predominantly in the Cu^I, TPQ semiquinone state. A new mechanistic proposal for O_2 reduction is advanced on the basis of thermodynamic considerations together with kinetic studies (at varying pH, temperature, and viscosity), the identification of steady-state intermediates, and the analysis of competitive oxygen kinetic isotope effects, ^{18}O KIEs, $[k_{cat}/K_M(^{16,16}O_2)]/[k_{cat}/K_M(^{16,18}O_2)]$. The ^{18}O KIE = 1.0136 ± 0.0013 at pH 7.2 is independent of temperature from 5 °C to 47 °C and insignificantly changed to 1.0122 ± 0.0020 upon raising the pH to 9, thus indicating the absence of kinetic complexity. Using density functional methods, the effect is found to be precisely in the range expected for reversible O_2 binding to Cu^I to afford a superoxide, $[Cu^{II}(\eta^1\text{-}O_2)^{-I}]^+$, intermediate. Electron transfer from the TPQ semiquinone follows in the first irreversible step to form a peroxide, $Cu^{II}(\eta^1\text{-}O_2)^{-II}$, intermediate driving the reduction of O_2. The similar ^{18}O KIEs reported for copper amine oxidases from other sources raise the possibility that all enzymes react by related inner-sphere mechanisms although additional experiments are needed to test this proposal.

I. Introduction

Copper amine oxidases[1] belong to a family of related quinoproteins which use molecular oxygen to effect oxidative deamination of primary amines to aldehydes and concomitantly produce hydrogen peroxide. The H_2O_2 is believed to have vital physiological as well as pathophysiological roles, particularly in cell signaling, inflammation, and diseases of the connective tissue.[2–4] The efficacy of H_2O_2 production is controlled by the enzyme's ability to mediate electron transfer from its reduced quinocofactor, which is derived from post-translational modification of an active site tyrosine.[1d] Remarkably, the enzymic rate of electron transfer to O_2 exceeds that of structurally analogous phenolic compounds in solution by several ($>10^5$) orders of magnitude.

As with many proteins that contain redox-active organic cofactors and metal ions, the origins of catalytic acceleration in reactions with O_2 have been a challenge to understand. The ambiguity in copper amine oxidase catalysis derives largely from an internal redox equilibrium which complicates assignment of the reactive form. Nevertheless, much effort has been devoted to studying the mechanisms of O_2 activation.[5] These investigations provide valuable insights as to the strategies used by enzymes to catalyze oxidations while avoiding damage by

---

* To whom correspondence should be addressed.
† Department of Chemistry, Johns Hopkins University.
‡ Department of Chemistry and Biochemistry, Montana State University.

(1) (a) Janes, S. M.; Mu, D.; Wemmer, D.; Smith, A. J.; Kaur, S.; Maltby, D.; Burlingame, A. L.; Klinman, J. P. *Science* **1990**, *248*, 981–987. (b) Wang, S. X.; Mure, M.; Medzihradszky, K. F.; Burlingame, A. L.; Brown, D. E.; Dooley, D. M.; Smith, A. J.; Kagan, H. M.; Klinman, J. P. *Science* **1996**, *273*, 1078–1084. (c) McIntire, W. S.; Hartmann, C. in *Principles and Applications of Quinoproteins*, Davidson, V. L., Ed.; Dekker: New York, 1993; pp 97−171. (d) Klinman, J. P. *Proc. Nat. Acad. Sci. USA* **2001**, *98*, 14766–14768. (e) Mure, M. *Acc. Chem. Res.* **2004**, *37*, 131–139.

(2) (a) Mondovi, B.; Pietrangeli, P.; Morpurgo, L.; Masini, E.; Federico, R.; Mateescu, M. A.; Befani, O.; Agostinelli, E. *Inflammopharmacology* **2003**, *11*, 155–163. (b) O'Sullivan, J.; Unzeta, M.; Healy, J.; O'Sullivan, M. I.; Davey, G.; Tipton, K. F. *Neurotoxicology* **2004**, *25*, 303–315. (c) Pietrangeli, P.; Mondovi, B. *Neurotoxicology* **2004**, *25*, 317–324. (d) Toninello, A.; Pietrangeli, P.; De Marchi, U.; Salvi, M.; Mondovi, B. *Biochim. Biophys. Acta, Rev. Cancer* **2006**, *1765*, 1–13. (e) O'Sullivan, J.; Davey, G.; O'Sullivan, M.; Tipton, K. F. *J. Neural Transmiss.* **2007**, *114*, 751–756.

(3) (a) Laurenzi, M.; Tipping, A. J.; Marcus, S. E.; Knox, J. P.; Federico, R.; Angelini, R.; McPherson, M. J. *Planta* **2001**, *214*, 37–45. (b) Rea, G.; De Pinto, M. C.; Tavazza, R.; Biondi, S.; Gobbi, V.; Ferrante, P.; De Gara, L.; Federico, R.; Angelini, R.; Tavladoraki, P. *Plant Phys.* **2004**, *134*, 1414–1426.

(4) (a) Harris, E. D.; O'Dell, B. L. *Adv. Exp. Med. Biol.* **1974**, *48*, 267–84. (b) Langford, S. D.; Trent, M. B.; Boor, P. J. *Cardiovasc. Toxicol.* **2002**, *2*, 141–150.

(5) (a) Klinman, J. P. *Acc. Chem. Res.* **2007**, *40*, 325–333. (b) Bollinger, J. M.; Krebs, C. *Curr. Opin. Chem. Biol.* **2007**, *11*, 151–158. (c) Decker, A.; Solomon, E. I. *Curr. Opin. Chem. Biol.* **2005**, *9*, 152–163. (d) *Active Oxygen in Biochemistry*; Valentine, J. S., Foote, C. S., Greenberg, A., Liebman, J. F., Eds.; Chapman & Hall: New York, 1995.
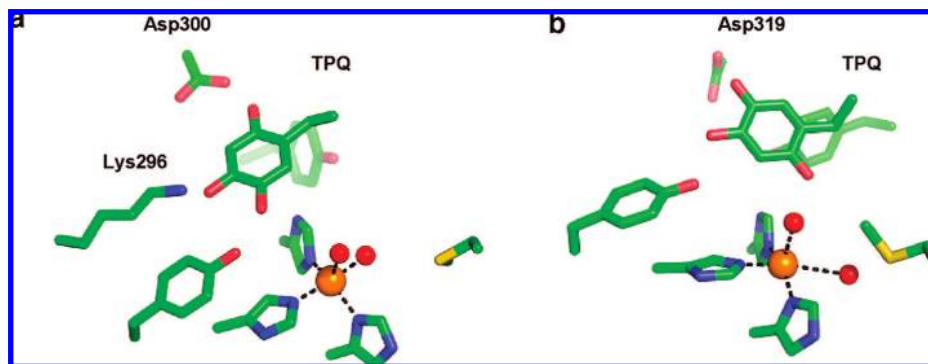
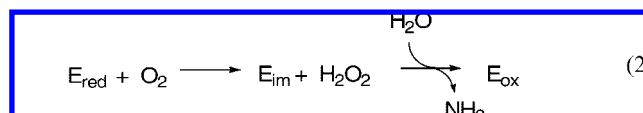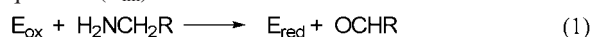**Figure 1.** Oxidized forms of copper amine oxidase from pea seedling[15] (a) and *H. polymorpha*[16] (b).

reactive oxygen species.[5a] The connection between oxidative damage and enzyme activity is becoming increasingly clear with copper-containing oxidases,[2,4,6] as well as superoxide dismutases,[7] being implicated in degenerative diseased states. The underlying mechanisms by which the enzymes are damaged possibly involve self-generated reactive oxygen species and remain only marginally understood.

In this work, we address the reductive activation of O_2 mediated by copper amine oxidase and the origins of the catalytic rates. In such metalloenzymes, O_2 reactivity can occur by either inner-sphere or outer-sphere electron transfer (ET) or combinations thereof. In inner-sphere ET, a bond between the redox metal and O_2 is formed in the transition state; whereas in outer-sphere ET, the reactant coordination geometries remain unchanged and $O_2^{\bullet-}$ is produced as an intermediate prior to its binding to the metal.[8] The coordination geometry of the metal and amino acids lining the active site influence the kinetic and thermodynamic barriers, which differentiate the ET pathways. Yet the factors that make one mechanism preferred over another have been difficult to define in the absence of the appropriate physical probes. Outlined in this study is the application of competitive oxygen kinetic isotope effects, together with density functional methods, as a potential solution to this problem.

The present study focuses specifically on the copper amine oxidase from pea seedling (PSAO) and the question of whether structurally homologous eukaryotic enzymes catalyze the reduction of O_2 to H_2O_2 by a common mechanism.[9] All members of the copper amine oxidase family contain a topaquinone (2,4,5-trihydroxyphenylalanine quinone, TPQ) cofactor in each homodimeric subunit. The TPQ is derived from oxidation of a specific tyrosine.[1] The self-processing reaction utilizes O_2 while exploiting the electronic structure of the copper ion and the hydrogen bond network of the active site,[10] factors which are also expected to influence the enzyme's catalytic reaction with O_2.

Catalysis in PSAO can be separated into kinetically independent reductive and oxidative half-reactions according to a ping-pong kinetic mechanism.[11] During the reductive phase (eq 1), two electrons are transferred from the amine to the oxidized enzyme (E_{ox}) which contains topaquinone, TPQ_{ox}, and Cu^{II}. This reaction involves conversion of a substrate Schiff-base to a product Schiff-base upon C−H deprotonation by a conserved aspartate residue.[12] Hydrolysis and product release afford the reduced enzyme (E_{red}) initially containing the aminoquinol TPQ_{red}, and Cu^{II}. This reduced state generates a neutral semiquinone, TPQ_{sq}, and Cu^I via an internal proton-coupled electron transfer. Equilibrium mixtures of TPQ_{sq}/Cu^I and TPQ_{red}/Cu^{II} are formed in enzymes from various sources with the

relative concentrations spanning a wide range. Data obtained in this study reveal that E_{red} in PSAO consists of ∼80% TPQ_{sq}/Cu^I at physiological pH (vide infra). This species, assuming its kinetic competence, would likely be involved in the oxidative phase of catalysis (eq 2), where two reducing equivalents are transferred from E_{red} to O_2 forming H_2O_2 and the enzyme iminoquinone (E_{im}).

$$E_{ox} + H_2NCH_2R \longrightarrow E_{red} + OCHR \qquad (1)$$

$$E_{red} + O_2 \longrightarrow E_{im} + H_2O_2 \xrightarrow[NH_3]{H_2O} E_{ox} \qquad (2)$$

The presence of electronically-coupled,[13] redox-active cofactors complicates the study of the O_2 reduction mechanism. Crystal structures[14–16] reveal that the Cu^{II} and TPQ_{ox} lie within ∼6 Å and are connected by hydrogen bonds which vary depending on the orientation of the organic cofactor. The two E_{ox} structures shown in Figure 1 are related by rotation of TPQ_{ox} 180° about $C_{\alpha}-C_{\beta}$. Only the HPAO structure is believed to be in a configuration conducive to the reductive half-reaction with Asp319 positioned to act as the catalytic base.[12] Whether the alternate structure is also favored in E_{red} of PSAO or capable of reacting with O_2 in the oxidative half-reaction has not been examined.

(6) (a) Xu, X.; Pin, S.; Gathinji, M.; Fuchs, R.; Harris, Z. L. *Ann. N.Y. Acad. Sci.* **2004**, *1012*, 299–305. (b) Mukhopadhyay, C. K.; Ehrenwald, E.; Fox, P. L. *J. Biol. Chem.* **1996**, *271*, 14773–14778.
(7) (a) Valentine, J. S.; Hart, P. J. *Proc. Nat. Acad. Sci. USA* **2003**, *100*, 3617–3622. (b) Valentine, J. S.; Doucette, P. A.; Potter, S. Z. *Annu. Rev. Biochem.* **2005**, *74*, 563–593. (c) Choi, J.; Rees, H. D.; Weintraub, S. T.; Levey, A. I.; Chin, L-S.; Li, L. *J. Biol. Chem.* **2005**, *280*, 11648–11655.
(8) Taube, H. *Prog. Inorg. Chem.* **1986**, *34*, 607–625.
(9) Pietrangeli, P.; Nocera, S.; Mondovi, B.; Morpurgo, L. *Biochim. Biophys. Acta, Proteins Proteom.* **2003**, *1647*, 152–156.
(10) Johnson, B. J.; Cohen, J.; Welford, R. W.; Pearson, A. R.; Schulten, K.; Klinman, J. P.; Wilmot, C. M. *J. Biol. Chem.* **2007**, *282*, 17767–17776.
(11) Yamasaki, E. F.; Swindell, R.; Reed, D. J. *Biochemistry* **1970**, *9*, 1206–1210.
(12) Mure, M.; Mills, S. A.; Klinman, J. P. *Biochemistry* **2002**, *41*, 9269–9278.
(13) Dooley, D. M.; McGuirl, M. A.; Brown, D. E.; Turowski, P. N.; McIntire, W. S.; Knowles, P. F. *Nature* **1991**, *349*, 262–264.
(14) Wilmot, C. M.; Hajdu, J.; McPherson, M. J.; Knowles, P. F.; Phillips, S. E. *Science* **1999**, *286*, 1724–1728.
(15) (a) Kumar, V.; Dooley, D. M.; Freeman, H. C.; Guss, J. M.; Harvey, I.; McGuirl, M. A.; Wilce, M. C. J.; Zubak, V. M. *Structure* **1996**, *4*, 943–955. (b) Duff, A. P.; Shepard, E. M.; Langley, D. B.; Dooley, D. M.; Freeman, H. C.; Guss, J. M. *Acta Crystallogr., Sect. F* **2006**, *62*, 1168–1173.
(16) Li, R.; Klinman, J. P.; Mathews, F. S. *Structure* **1998**, *6*, 293–307.

The intricate hydrogen-bonding within the copper amine oxidase active sites might facilitate coupled movements of electrons and protons in a single step. This type of proton-coupled electron transfer reaction can lower barriers to redox processes that would otherwise require formation of high-energy, charged intermediates. In PSAO, the rapid oxidation of TPQ_{red} by Cu^{II} results in an equilibrium (K_{int}) that is established on the time scale of microseconds.[17] As a result, the TPQ_{sq}/Cu^I state is kinetically competent to sustain catalysis in this enzyme. In this potentially reactive state, the TPQ_{sq} is inert to oxygenation while the Cu^I is expected to be highly reactive toward O_2.[18]

This is, to the best of our knowledge, the first detailed mechanistic investigation of O_2 activation in PSAO. Attempts to correlate the steady-state kinetics to the internal redox equilibrium within E_{red} are described as are experiments that probe the contributions of proton and electron transfer to the observed bimolecular rate constant, $k_{cat}/K_M(O_2)$. The contribution of common steps within $k_{cat}/K_M(O_2)$ and k_{cat} is examined through the analysis of substrate deuterium kinetic isotope effects and the intermediates which accumulate during steady-state turnover with fast and slow substrates.

Competitive oxygen kinetic isotope effects (^{18}O KIEs) on reactions of natural abundance O_2, $k_{cat}/K_M(^{16,16}O_2)/k_{cat}/K_M(^{16,18}O_2)$, are prominently featured in this study. These values have been difficult to explain in earlier studies of copper amine oxidase, raising questions concerning the mechanism of the oxidative half-reaction as well as the physical origins of the [18]O KIEs.[12,19,20] Here, the isotope effects are interpreted in light of extensive density functional calculations using methods we have recently established by benchmarking calculated values against those experimentally determined for structurally defined, synthetic copper—oxygen compounds.[21] The difficulties encountered in earlier works are discussed and the [18]O KIEs are shown to fall precisely within the computationally derived limits. We believe that this combined experimental/computational approach[22] holds great promise for characterizing intermediates in metalloenzymes which activate O_2 as well as those which process reactive oxygen species ($O_2{}^{\bullet-}$ and H_2O_2) using metal cofactors.

II. Experimental Section

General. PSAO was isolated in ~98% purity following a previously described method.[23] Specialty chemicals were obtained from Sigma in the highest purity available unless noted otherwise. Substrate stock solutions were prepared from putrescine (1,4-diaminobutane) in its free base or dihydrochloride form. Putrescine with all carbons deuterium-labeled (1,4-butane-d_8-diamine dihydrochloride and 1,4-butane-d_8-diamine) 99.5% and α,α-d_2-benzylamine 99% were purchased from C/D/N Isotopes. The

percent protio contamination was confirmed to be between 0.4 and 0.6% by ^{1}H NMR (Varian Unity Inova 500 Mhz).

1. Spectrophotometric Measurements. Spectrophotometry was performed using an 8452 or 8453 diode array system (Agilent), a Cary 6000i (Varian) or a RSM1000 stopped-flow (OLIS). Optical spectra were recorded under a rigorously anaerobic atmosphere at 25 °C unless noted otherwise. Conventional spectrophotometry was performed using resealable quartz cells (Starna). Stopped-flow measurements were performed inside a glovebox (MBraun). Enzyme solutions were degassed through multiple cycles of vacuum and nitrogen or vacuum and argon. Titration experiments were performed by adding substrates using a glovebox or standard Schlenk techniques. The concentration of oxidized enzyme, containing two quinocofactors per mole of protein, was determined from the absorbance due to TPQ_{ox}. The TPQ_{ox} has an extinction coefficient of $\epsilon_{495nm} = 2450$ $M^{-1}cm^{-1}$ (per monomer) at pH 7.2.[23] On this basis, the extinction coefficient of the semiquinone form of the enzyme was determined to be $\epsilon_{465nm} = 7000$ M^{-1} cm^{-1} (per monomer).[24]

2. Steady-State Kinetics. Measurements of initial O_2 consumption rates at steady-state were performed using a Clark-type oxygen electrode (Yellow Springs Inc.; 5300 A voltmeter and 5331 A probe). The ionic strength was maintained at 0.1 ± 0.02 M at varying pH. Chloride was introduced as a counterion for the protonated amine substrate in some experiments with no discernible effect. It was thus confirmed that Cl^- does not inhibit putrescine oxidation or O_2 reduction by PSAO.[25]

A standard assay was developed to check the enzyme concentrations. An air-saturated solution containing ~272 μM O_2 and 5 mM putrescine at pH 7.2 was used, where $v/[E]_T$ (22 °C) = 197 s^{-1} per dimer, i.e., 98.5 s^{-1} per monomer. The protein concentration was determined from the absorbance of TPQ_{ox} at 495 nm as well as its absorbance after titration with phenylhydrazine. Phenylhydrazine titrations indicated the presence of 1.6−2.0 equiv of TPQ per dimer in all batches of protein. The concentration of active enzyme was additionally checked by comparison to the established specific activity with benzylamine.[23] Initial rates were confirmed to vary, as expected, in proportion to the enzyme concentration. Change in enzyme activity at the extremes of pH and temperature was monitored by preincubating stock solutions (1−10 min) under the relevant conditions followed by a standard assay.

Kinetic data were collected between 5 °C and 50 °C using the O_2 electrode in a water jacketed reaction chamber equipped with a recirculating bath (VWR 116−0S). Reaction solutions were typically pre-equilibrated for several minutes against varying mixtures of O_2 and N_2 at 1 atm prior to initiating the reaction by addition of the enzyme (2.5−80 nM). Initial rates of O_2 uptake exceeded the electrode's background drift rate by at least a factor of 10. The enzymatic rate was calculated from the most linear portion of the decay curve approximately 10 s after mixing of the enzyme and substrate solutions.

Initial rate data at varying substrate concentrations were analyzed using Kaleidagraph 4.0 (Synergy Software). Kinetic parameters were obtained by fitting at least ten points to the Michaelis—Menten expression (eq 3); v is the initial rate, $[E]_T$ is the total active enzyme concentration, $^{ap}K_M$ is the apparent Michaelis constant and $^{ap}k_{cat}$ is the apparent rate constant for enzyme turnover. The limiting k_{cat}, K_M and k_{cat}/K_M values are reported with 2σ errors derived from the nonlinear curve-fitting analysis.

(17) Turowski, P. N.; McGuirl, M. A.; Dooley, D. M. *J. Biol. Chem.* **1993**, *268*, 17680–17682.

(18) Cramer, C. J.; Tolman, W. B. *Acc. Chem. Res.* **2007**, *40*, 601–608.

(19) Roth, J. P. *Curr. Opin. Chem. Biol.* **2007**, *11*, 142–150.

(20) (a) Prabhakar, R.; Siegbahn, P. E. M.; Minaev, B. F.; Agren, H. *J. Phys. Chem. B* **2004**, *108*, 13882–13892. (b) Prabhakar, R.; Siegbahn, P. E. M.; Minaev, B. F. *Biochim. Biophys. Acta, Proteins Proteom.* **2003**, *1647*, 173–178.

(21) Lanci, M. P.; Smirnov, V. V.; Cramer, C. J.; Gauchenova, E. V.; Sundermeyer, J.; Roth, J. P. *J. Am. Chem. Soc.* **2007**, *129*, 14697–14709.

(22) For a leading review that describes the application of heavy atom kinetic isotope effects together with DFT methods, see: Schramm, V. L. *J. Biol. Chem.* **2007**, *282*, 28297–28300.

(23) McGuirl, M. A.; McCahon, C. D.; McKeown, K. A.; Dooley, D. M. *Plant Physiol.* **1994**, *106*, 1205–1211.

(24) (a) Medda, R.; Padiglia, A.; Bellelli, A.; Pedersen, J. Z.; Finazzi-Agro, A.; Floris, G. *FEBS Lett.* **1999**, *453*, 1–5. (b) Medda, R.; Mura, A.; Longu, S.; Anedda, R.; Padiglia, A.; Casu, M.; Floris, G. *Biochimie* **2006**, *88*, 827–835, The extinction coefficient of the TPQ_{sq} determined in this study is based on the extinction coefficient of TPQ_{ox} (at pH 7.2 and 22 °C). This value of TPQ_{ox} is similar among enzymes from different sources according to ref 12.

(25) Juda, G. A.; Shepard, E. M.; Elmore, B. O.; Dooley, D. M. *Biochemistry* **2006**, *45*, 8788–8800.

$$\frac{v}{[E]_T} = \frac{^{ap}k_{cat}[S]}{^{ap}K_M + [S]} \quad (3)$$

a. Kinetics at Varying pH. The following buffers were used to study the kinetics at varying pH: 0.1000 M MES (2-(N-morpholino)ethane sulfonic acid) at pH 5.2, 0.0850 M sodium phosphate at pH 6, 0.0500 M sodium phosphate at pH 7.2, 0.0160 M sodium pyrophosphate at pH 8, 0.0136 M sodium pyrophosphate at pH 9, 0.0107 M sodium pyrophosphate at pH 10. The ionic strength was maintained at 0.1 ± 0.02 M by varying the buffer concentration. The absence of specific buffer effects was confirmed by comparing $k_{cat}/K_M(O_2)$ in two different buffers at the same pH and ionic strength; for example, MES and phosphate buffer at pH 6.2 gave indistinguishable results.

b. Solvent Isotope Effect Studies. Deuterated buffer solutions were prepared as outlined above using salts enriched by dissolution in D_2O (99.9% Cambridge Isotope Laboratories) and evaporation to dryness. Solution pH and pD values (pD = pH$_{reading}$ + 0.4) were determined using an Accumet Research pH meter at 22 °C. Small corrections of -0.0028 unit/°C (phosphate) and 0.01 unit/°C (pyrophosphate) were applied above and below room temperature. Solvent isotope effects are reported as the average of at least three measurements with the errors propagated according to eq 4; $k_H = [k_{cat}/K_M(O_2)]_{H_2O}$, $k_D = [k_{cat}/K_M(O_2)]_{D_2O}$ and $\Delta k_{H \text{ or } D}$ corresponds to the standard error from the nonlinear regression analysis.

$$\Delta\left(\frac{k_H}{k_D}\right) = \sqrt{\left(\frac{1}{k_D}\right)^2 (\Delta k_H)^2 + \left[\frac{-k_H}{(k_D)^2}\right]^2 (\Delta k_D)^2} \quad (4)$$

c. Substrate Deuterium Kinetic Isotope Effect Studies. Deuterium kinetic isotope effects were measured by comparing rate constants obtained with d$_8$-putrescine or α,α-d$_2$-benzylamine with those of the corresponding per-protio substrates. Errors were propagated as described above; in Eq 4, k_H and k_D for the protio and deutero substrates, respectively, are associated with either k_{cat} or k_{cat}/K_M. The uncompetitively determined kinetic isotope effects are reported conservatively with errors of $\pm 2\sigma$.

d. Viscosity Effects. Experiments to probe contributions from diffusion to k_{cat}/K_M were conducted using sucrose or glycerol as the solvent viscosogen. Solution viscosities were determined relative to a buffer-only solution using an Ostwald viscometer at 22 °C. Data were analyzed per the relationship: $[k_{cat}/K_M(O_2)]^0/[k_{cat}/K_M(O_2)] = (\eta/\eta^0)^{exp}$; the "0" designates the absence of viscosogen. According to the Stokes–Einstein relation, an exponent of 1 should be observed for diffusion-limited binding of the amine substrate or diffusion-limited dissociation of the aldehyde product.[26] A smaller, empirically determined exponent of 0.5 has been proposed to describe deviations from Stokes–Einstein behavior for small diatomic solutes like O_2.[27]

3. Competitive Oxygen Kinetic Isotope Effects. Oxygen kinetic isotope effects (^{18}O KIEs) were determined using a previously described competitive technique and a home-built high vacuum apparatus.[28] Natural abundance O_2 was used in these experiments. Analysis performed by isotope ratio mass spectrometry (IRMS) afforded the $^{18}O/^{16}O$ content of CO_2 samples, which were prepared by quantitatively combusting the O_2 isolated from solutions before and after introducing PSAO.

^{18}O KIE measurements were performed over a range of temperatures (at 5, 22, or 47 °C) in substrate-containing solutions (pH 7.2 or 9.0). In these experiments, putrescine-containing solutions were saturated with O_2 or He/O_2 mixtures and then loaded into an injectable glass reaction chamber. The chamber was equipped with a movable piston and two-way crossover stopcock for sampling the solution. Connection of the chamber to the vacuum apparatus allowed fixed volumes of the reaction solution (typically 10 mL) to be withdrawn in vacuo at varying stages of reaction. No O_2 consumption was detectable when putrescine-containing solutions were allowed to stand for $1-3$ h in the absence of enzyme. Reactions were initiated by injecting a solution of PSAO through a resealable septum. The enzymatic reaction was quenched prior to removing the O_2 by addition of 5-sulfosalicylic acid (20 mg) in 0.5 mL 85% H_3PO_4. Samples were prepared after isolating the O_2 from other condensable gases. The O_2 was quantitatively converted to CO_2 by combustion over graphite with platinum wire at 900 °C. CO_2 samples were condensed into dry glass tubes and flame sealed after determining the pressure of gas using a capacitance manometer (Omega PX238). The precision of the pressure measurements was typically $\pm 3\%$ with the CO_2 related to the fractional consumption of O_2 by the enzymatic reaction.

IRMS analysis of CO_2 samples was achieved using a dual-inlet, stable isotope ratio mass spectrometer in the Environmental Isotope Laboratory at the University of Waterloo (Ontario, Canada). The $^{18}O/^{16}O$ in samples prepared using the procedure outlined above was precise to ± 0.0003. The isotope fractionation of the unreacted O_2 was interpreted using eq 5 which expresses the ^{18}O KIE in terms of a ratio of ratios; i.e., the $^{18}O/^{16}O$ (R_f) at a specific fractional conversion (f) relative to the $^{18}O/^{16}O$ (R_0) prior to the enzymatic reaction. The ^{18}O KIEs reported in this work were determined at fractional conversions from 5% to 55% by solving eq 5. The KIE is quoted as the average of at least five independent measurements with errors quoted as $\pm 1\sigma$ about the mean.

$$^{18}\text{O KIE} = \left[1 + \frac{\ln(R_f/R_0)}{\ln(1-f)}\right]^{-1} \quad (5)$$

4. Density Functional Calculations. Calculations at the density functional level of theory (DFT) were performed using *Gaussian 03W*.[29] Molecular geometries were optimized with the *m*PWPW91 functional[30] and the following atomic orbital basis functions:[31] CEP-31G for Cu,[32] 6-311G* for N and O, 6-31G for C, and STO-3G for H. Complexes formally assigned as copper(II) end-on (η^1) superoxide species were assumed based on previous results[21] to have triplet ground states. The end-on (hydro)peroxide or side-on (η^2) peroxide species have doublet ground states. Calculations on these states were thus performed using unrestricted Kohn–Sham (KS) DFT.[33] The stability of KS self-consistent field solution was confirmed for each optimized structure. Molecular orbitals were visualized for all structures and the singly occupied molecular orbitals (SOMOs) confirmed to be associated with copper and/or dioxygen.

To match the active site structure of PSAO as well as compare structures with differing sterics and electronics about Cu^{II}, DFT calculations were performed with imidazole or methylimidazole as supporting ligands. In one set of calculations the methylimidazole was constrained to interact through the δ-imino rather than the ϵ-imino nitrogen, as seen in the published crystal structure of PSAO.[15] Vibrational frequencies were calculated analytically for each optimized structure within the harmonic oscillator approximation.[33] All minima were characterized by real frequencies in all

(26) Brouwer, A. C.; Kirsch, J. F. *Biochemistry* **1982**, *21*, 1302–1307.

(27) (a) Hasinoff, B. B.; Chishti, S. B. *Biochemistry* **1982**, *21*, 4275–4278. (b) Dunford, H. B.; Hasinoff, B. B. *J. Inorg. Biochem.* **1986**, *28*, 263–269.

(28) (a) Roth, J. P.; Klinman, J. P. in *Isotope Effects in Chemistry and Biology*; Kohen, A., Limbach, H.-H., Eds.; CRC Press: Boca Raton, 2006; pp 645–669. (b) Smirnov, V. V.; Brinkley, D. W.; Lanci, M. P.; Karlin, K. D.; Roth, J. P. *J. Mol. Catal. A.* **2006**, *251*, 100–107.

(29) Frisch, M. J.; et al. *Gaussian 03*, revision C.02; Gaussian, Inc.: Wallingford, CT, 2004.

(30) Perdew, J. P.; Wang, Y. *Phys. Rev. B* **1986**, *33*, 8800–8802. Perdew, J. P. in *Electronic Structure of Solids '91*; Ziesche, P., Eschrig, H., Eds.; Akademie Verlag: Berlin, 1991; pp 11–20. Adamo, C.; Barone, V. *J. Chem. Phys.* **1998**, *108*, 664–675.

(31) Hehre, W. J.; Radom, L.; Schleyer, P. R.; Pople, J. A. *Ab Initio Molecular Orbital Theory*; Wiley: New York, 1986.

(32) Stevens, W. J.; Krauss, M.; Basch, H.; Jasien, P. G. *Can. J. Chem.* **1992**, *70*, 612–629.

(33) Cramer, C. J. *Essentials of Computational Chemistry* 2nd Ed., Wiley: Chichester, 2004.
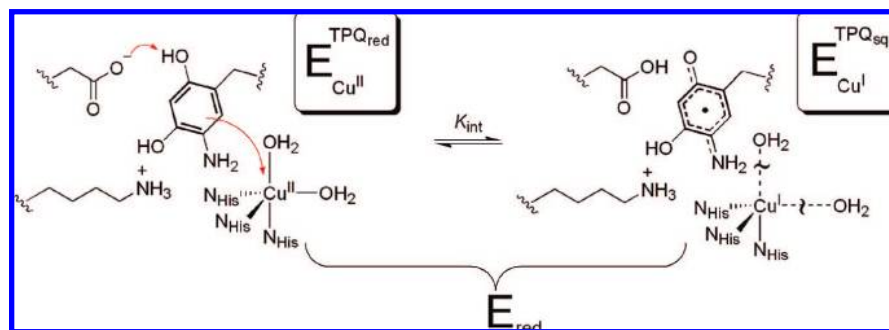
Figure 2. Redox equilibrium in reduced PSAO (E_{red}) involving proton-coupled electron transfer.
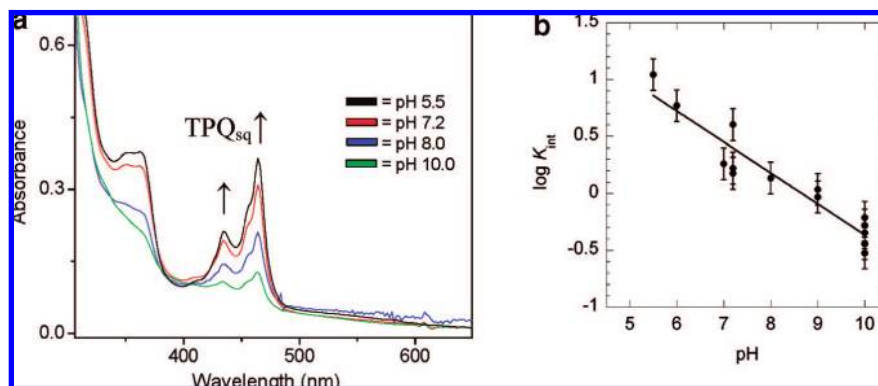

Figure 3. (a) Redox titration of PSAO showing formation of TPQ_{sq} under anaerobic conditions. (b) The pH dependence of K_{int} (cf. Figure 2) corresponding to production of $E(Cu^I, TPQ_{sq})$ at 22 °C, $\mu = 0.1$ M.

but a few cases where imaginary frequencies (from 4 to 9 cm^{-1}) with negligible isotope shifts were observed.

We recently established a density functional method to reproduce experimentally determined oxygen equilibrium isotope effects (^{18}O EIEs).[21] The latter study demonstrated the need for using full sets of stretching frequencies associated with the ^{16}O–^{16}O and ^{16}O–^{18}O isotopologues of the reactant and product states in the calculations. We apply this established computational method again using the Bigeleisen and Goeppert–Mayer formalism to calculate ^{18}O EIEs.[21,34] Certain calculations were performed on structures where O$_2$ binds to copper in an asymmetric manner. As previously demonstrated, neglecting the small intramolecular isotope effect, by assuming a 50/50 average of Cu^{16}O–^{18}O and Cu^{18}O–^{16}O structures, has an insignificant effect on the calculated ^{18}O EIE.[21]

Studies of ^{18}O EIEs have indicated that the effects can exhibit significant variations with temperature depending on the population of isotopically sensitive low frequency modes.[21] Therefore, in this study the temperature dependence of the ^{18}O EIEs was carefully evaluated for each of the calculated structures. In most cases, it was determined that the ^{18}O EIEs at 22 °C were indistinguishable from the maximum ^{18}O EIE, which generally occurs at a lower temperature.

III. Results

A. Identity of the Resting Reduced Enzyme. PSAO was reduced anaerobically to probe the equilibrium between the two states: $E(Cu^{II}, TPQ_{red})$ and $E(Cu^I, TPQ_{sq})$ (K_{int} in Figure 2). Experiments were performed by treating the enzyme-containing solution with the substrate (putrescine, *N,N*-dimethylaminomethylbenzylamine or benzylamine) under an O$_2$-free atmosphere. Conventional mixing and rapid-mixing techniques were employed to generate equilibrium mixtures. K_{int} was determined from the absorbance due to the TPQ_{sq} and the initial TPQ_{ox}. The results were found to be independent of the protein preparation as well as the presence of excess amine.

The pH dependence of K_{int} was investigated at 22 °C. The end-point was confirmed by the absence of spectral change upon addition of excess substrate or by addition of sodium cyanide (NaCN) which shifts the equilibrium to favor the enzyme-bound semiquinone, i.e., the $E(Cu^I, TPQ_{sq})$ state.[13,35,36] The TPQ_{red} has an insignificant extinction coefficient between 450 and 500 nm;[12] therefore, its absorbance contribution was neglected. Titration of the protein with phenylhydrazine corroborated the results and indicated that all of the TPQ_{ox} was present in an amine-reactive form.

The optical spectra at varying pH report on the protonation states of the TPQ species in PSAO. The absorbance due to TPQ_{ox} blue shifts from 508 to 485 nm as the pH is raised from 6 to 10, most likely due to deprotonation of the hydroxyl group in the 2 or 4 position.[37] The absence of a pH-dependent variation in the TPQ_{sq} optical spectrum suggests that this species exists in its neutral form (Figure 3a). Since the optical bands at 434 and 465 nm arise from the vibronic structure of the TPQ_{sq},[38] they would be expected to change upon cofactor protonation. The observed behavior is as expected on the basis of solution studies where the semiquinone radical cation of 4-aminoresorcinol exhibits a pK_a of 3.4.[39] Although unobservable in PSAO, partial deprotonation of the neutral TPQ_{red} and TPQ_{sq} would be expected at sufficiently high pH in view of model studies which revealed a pK_a of 9.59 for 6-amino-4-ethylresorcinol.[37]

(34) Details are provided as Supporting Information.
(35) Shepard, E. M.; Juda, G. A.; Ling, K-Q.; Sayre, L. M.; Dooley, D. M. *J. Inorg. Biochem.* **2004**, *9*, 256–268.
(36) Welford, R. W. D.; Lam, A.; Mirica, L. M.; Klinman, J. P. *Biochemistry* **2007**, *46*, 10817–10827.
(37) Mure, M.; Klinman, J. P. *J. Am. Chem. Soc.* **1993**, *115*, 7117–7127.
(38) Tripathi, G. N. R. *J. Chem. Phys.* **2003**, *118*, 1378–1391.
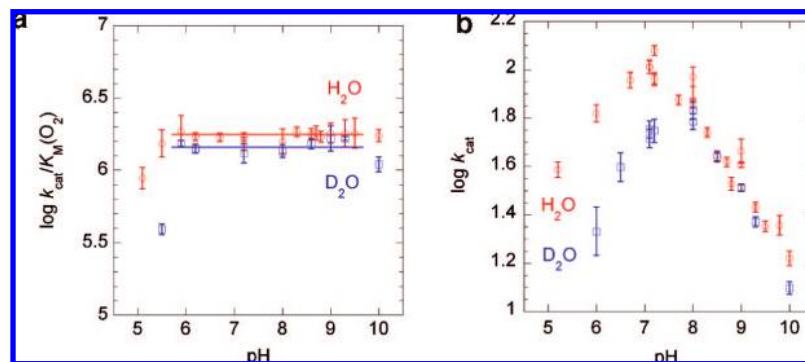(39) Bisby, R. H.; Johnson, S. A.; Parker, A. W. *J. Phys. Chem. B* **2000**, *104*, 5832–5839.

Figure 4. Profiles of (a) $k_{cat}/K_M(O_2)$ and (b) k_{cat} at 22 °C (H$_2$O, red circles), (D$_2$O, blue squares). The ionic strength was maintained in all experiments (μ = 0.1 M).

The spectrophotometric titration results indicate that K_{int} weakly depends upon the solution pH (Figure 3b). The fraction of E(Cu^I, TPQ$_{sq}$) *increases* approximately 4-fold upon *lowering* the solution pH from 10 to 5. These results are opposite to those which would be expected to accompany protonation of the anionic or neutral TPQ$_{red}$, where changing the pH by one unit should decrease the concentration of E(Cu^I, TPQ$_{sq}$) relative to E(Cu^{II}, TPQ$_{red}$) by a factor of 10 (1 log unit in K_{int}). The results can alternatively be explained by protonation of peripheral residues. Increasing the positive charge in the active site may increase the Cu$^{II/I}$ redox potential, favoring K_{int}. The titration results clearly show that, at physiological pH and 22 °C, the reduced enzyme exists largely (~80%) in the E(Cu^I, TPQ$_{sq}$) form. This result would impact the interpretation of the kinetic data if the reaction of E$_{red}$ with O$_2$ were rate-determining.

B. Kinetics of the Oxidative Half-Reaction. 1. pH and pD Profiles. The spectroscopic redox titration results are in marked contrast to the O$_2$-dependent kinetics. The $k_{cat}/K_M(O_2)$ at 22 °C is unchanged between pH 6.0 and 9.5 (Figure 4a). The average $k_{cat}/K_M(O_2)$ in D$_2$O is slightly lower than in H$_2$O over the same pD range suggesting a small solvent isotope effect of 1.2 ± 0.2. The effect is consistent with a prototropic pre-equilibrium and the absence of rate-determining proton transfer from a solvent-exchangeable site.

Below pH 6, there is a falloff in rate constant that is more pronounced in D$_2$O than in H$_2$O. The observed behavior is consistent with a protonation event that deactivates the enzyme. It is tempting to associate this event with formation of the cationic TPQ$_{red}$, but a parallel change in the concentration of the E(Cu^I,TPQ$_{sq}$) is not seen in the spectrophotometric redox titrations at low pH. Instead, the concentration of E(Cu^I,TPQ$_{sq}$) increases monotonically to ~90%. The results indicate that the intrinsic pK_a values, such as those associated with a copper-bound water molecule or TPQ cofactor, cannot be discerned from the kinetics. Such behavior can occur when complex equilibria precede the irreversible step (vide infra).[40] At this stage, the only conclusion that can be drawn from the different pH profiles of $k_{cat}/K_M(O_2)$ and k_{cat} is that the two parameters do not share a common irreversible step.

2. Solvent Viscosity Studies. The dependence of $k_{cat}/K_M(O_2)$ upon solution viscosity was examined to address whether the bimolecular rate constant contains a step controlled by the diffusion of O$_2$. Experiments were performed at relative viscosities, η/η^0 from 4.1 to 5.1. Such high relative viscosities

(40) (a) Cleland, W. W. *Adv. Enzymol. Relat. Areas Mol. Biol.* **1977**, *45*, 273–387. (b) Renard, M.; Fersht, A. R. *Biochemistry* **1973**, *12*, 4713–4718.
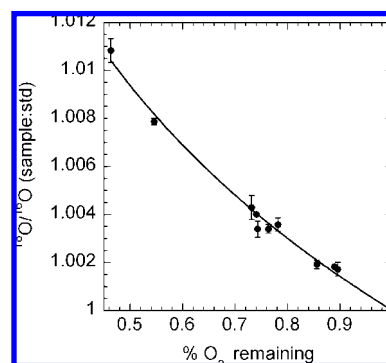
Figure 5. Oxygen isotope fractionation during PSAO turnover at pH 7.2 and 22 °C, μ = 0.1 M.

are needed to observe an effect in cases where small solutes like O$_2$ are involved and show deviations from ideal Stokes–Einstein behavior.[27] No sign of a viscosity effect was detectable at pH 7.2 and 22 °C, indicating the absence of an encounter-controlled reaction. The $k_{cat}/K_M(O_2)$ determined in the presence of glycerol (2.3 ± 0.3 × 10^6 M^{-1}s^{-1}) or sucrose (2.5 ± 0.2 × 10^6 M^{-1}s^{-1}) is slightly increased from the $k_{cat}/K_M(O_2)$ in the absence of viscosogen (2.1 ± 0.2 × 10^6 M^{-1}s^{-1}), suggesting small nonspecific effects of the viscosogen on the protein structure. Such nonspecific effects primarily impact k_{cat}, which changes from 99 ± 2 s^{-1} in buffer-only solutions to 72 ± 2.5 in the presence of glycerol (η/η^0 = 4.1– 5.2) and 147 ± 20 s^{-1} in the presence of sucrose (η/η^0 = 4.5). Control experiments revealed that k_{cat}/K_M(putrescine) = 8.5 ± 0.2 × 10^5 M^{-1}s^{-1} is characterized by a small positive viscosity effect upon addition of glycerol (slope of 0.20 ± 0.11) suggesting partial rate-limitation by substrate binding.

3. Oxygen Kinetic Isotope Effects. The ^{18}O KIE corresponding to $[k_{cat}/K_M(^{16,16}O_2)]/[k_{cat}/K_M(^{16,18}O_2)]$ is readily determined using a competitive isotope fractionation technique and natural abundance O$_2$.[28] As outlined above, the reaction mixture is sampled at different stages to probe the changes in the ^{18}O/^{16}O as the reaction progresses. During PSAO catalysis, the heavier isotopologue accumulates in the unreacted O$_2$ due to the faster reaction of ^{16}O–^{16}O than ^{18}O–^{16}O and a normal ^{18}O KIE is observed. Data obtained using different preparations of PSAO and amine cosubstrates are shown fitted to the isotope fractionation expression (eq 5) to illustrate the precision of the competitive ^{18}O KIE measurements (Figure 5).

Experiments at pH 7.2 indicate an ^{18}O KIE = 1.0136 ± 0.0014 at 22 °C. The isotope effect is independent of the O$_2$ consumed, as expected for a reaction where the contribution of
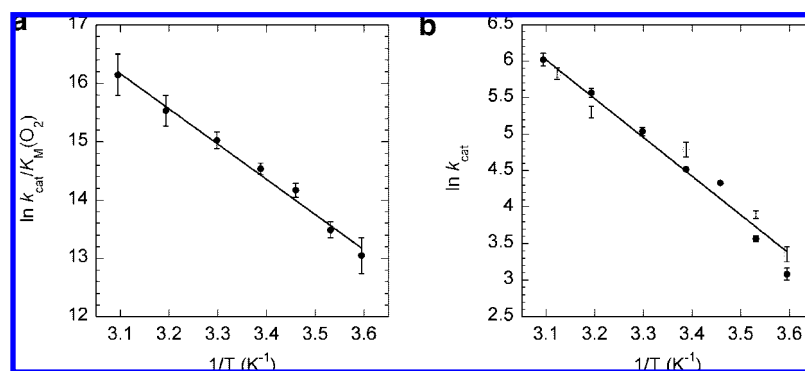
Figure 6. Activation parameters for putrescine oxidation at pH 7.2 ($\mu = 0.1M$): (a) the temperature dependence of (a) $k_{cat}/K_M(O_2)$ and (b) k_{cat}. The k_{cat} values were determined by varying amine (open circles) or varying O_2 (closed circles). Error bars correspond to $\pm 2\sigma$.

the isotopically sensitive step to $k_{cat}/K_M(O_2)$ remains unchanged. The [18]O KIE is also independent of H_2O_2 accumulation during the reaction as indicated by the lack of effect upon adding horseradish peroxidase and a sacrificial reductant, either guaiacol or ferrocyanide, to scavenge the H_2O_2 from reaction solutions.

Importantly, the isotope fractionation experiments performed over a range of conditions provide no evidence for a change in the step which limits $k_{cat}/K_M(O_2)$. The [18]O KIE at pH 9 and 22 °C, 1.0122 ± 0.0020, is the same within experimental error of that quoted above for pH 7.2. The pH 7.2 data are independent of temperature falling within the narrow range of 1.0133 ± 0.0017 at 5 °C and 1.0140 ± 0.0010 at 47 °C. These results appear to exclude kinetic complexity allowing rigorous analysis of the [18]O KIEs using DFT methods. In addition, the temperature invariant [18]O KIEs support the interpretation of the activation parameters determined for $k_{cat}/K_M(O_2)$ over the same range.

C. Deuterium Kinetic Isotope Effects on Amine Oxidation. Substrate deuterium kinetic isotope effects were determined to assess the contribution from C–H cleavage to k_{cat} and, consequently, the relative extents to which the oxidative and reductive half-reactions limit enzyme turnover. Uncompetitive deuterium KIEs ($^Dk_{cat}$ and $^Dk_{cat}/K_M$) were analyzed with putrescine and benzylamine; these fast and slow substrates exhibit rate constants that vary by more than 10^2 at pH 7.2 and 22 °C. In experiments at saturating levels of O_2, partially rate-limiting C–H cleavage was indicated for both substrates: $^Dk_{cat}$(putrescine) = 4.1 ± 0.2 and $^Dk_{cat}/K_M$(putrescine) = 3.3 ± 0.6 and benzylamine: $^Dk_{cat}$(benzylamine) = 2.3 ± 0.2 and $^Dk_{cat}/K_M$(benzylamine) = 9.5 ± 1.6.

Differences in the extent to which C–H cleavage is rate-limiting were further observed upon varying the pH. $^Dk_{cat}$ for putrescine was 4.2 ± 0.4 at pH 8 and 3.4 ± 0.2 at pH 10. In contrast, $^Dk_{cat}/K_M$(putrescine) decreased dramatically from 9.2 ± 1.0 to 1.1 ± 0.4 as the pH was varied from 6 to 10. These results are consistent with a common irreversible step in k_{cat} and k_{cat}/K_M(putrescine) changing from one dominated by C–H deprotonation to one dominated by formation of the substrate Schiff-base.

The temperature dependence of the deuterium KIE upon putrescine oxidation was examined at pH 7.2 under the same conditions used to determine the activation parameters for k_{cat} and $k_{cat}/K_M(O_2)$. The $^Dk_{cat}$ increased from 3.3 ± 0.2 at 5 °C to 5.1 ± 0.2 at 47 °C. These values are significantly below the intrinsic isotope effect, which is estimated to be ∼9.2 on the basis of the above-mentioned measurements at low pH. The trend with temperature is opposite that expected for a primary kinetic isotope effect determined largely by the influence of zero

point energy on the activation barrier.[41] Instead, the variation in $^Dk_{cat}$ arises from an increase in the extent to which C–H cleavage is rate-limiting at high temperatures. Thus, k_{cat} consists of multiple steps with C–H cleavage contributing by ∼35 to 55%. The dissociation of the product aldehyde and the release of H_2O_2 are also possible contributors to this kinetic parameter.

D. pH/pD Dependence of k_{cat}(putrescine). The pH and pD profiles of k_{cat}(putrescine) resemble those previously published for other eukaryotic amine oxidases (Figure 4b).[42–44] The limiting rate constants obtained from experiments at varying amine or O_2 are poorly fitted by two and three pK_a models. This observation is not surprising since k_{cat}(putrescine) is a kinetically complex parameter, as demonstrated by the evaluation of $^Dk_{cat}$ as a function of pH and temperature. The pH dependence of k_{cat} is less complex in the low pH regime where apparent pK_a values of 5.2 (H_2O) and 6.0 (D_2O) are observed together with a variation of 1 order of magnitude in rate per pH unit. This behavior is consistent with ionization of the active site Asp within the substrate Schiff-base complex.[12] In the basic regime, k_{cat} in H_2O and D_2O are indistinguishable within the limits of error. Control experiments indicate that the diminished rate constant does not arise from irreversible denaturation of the protein suggesting the presence of a high pH form of the enzyme with lower overall activity.

E. Thermal Activation Parameters. Steady-state kinetic parameters were evaluated at pH 7.2 at several temperatures between 5 °C and 50 °C (Figure 6). In spite of the kinetic complexity, the temperature dependence of k_{cat} (Figure 6b) is characterized by a relatively linear Arrhenius plot with $E_{act} = 10.5 \pm 1.2$ kcal mol^{-1} and $A = (5.7 \pm 3.9) \times 10^9$ s^{-1}. The $\Delta H^{\ddagger} = 9.9 \pm 1.1$ kcal mol^{-1} and $\Delta S^{\ddagger} = -14.8 \pm 2$ e.u. are obtained by assuming a pre-exponential frequency factor of 10^{13} s^{-1}. These activation parameters reflect multiple unimolecular steps including C–H deprotonation.

The Arrhenius plot of $k_{cat}/K_M(O_2)$ versus temperature (Figure 6a) is also linear with $E_{act} = 12.0 \pm 1.1$ kcal mol^{-1}. A surprisingly large Y-intercept indicates a pre-exponential term of $A = (1.4 \pm 1.5) \times 10^{15}$ M^{-1}s^{-1}. Assuming an adiabatic pre-exponential frequency factor of 10^{11} M^{-1}s^{-1},[45] the activa-

(41) Melander, L.; Saunders, W. H., Jr. *Reaction Rates of Isotopic Molecules* Wiley & Sons: New York, 1980; p 22.
(42) Mills, S. A.; Goto, Y.; Su, Q.; Plastino, J.; Klinman, J. P. *Biochemistry* **2002**, *41*, 10577–10584.
(43) Pietrangeli, P.; Federico, R.; Mondovi, B.; Morpurgo, L. *J. Inorg. Biochem.* **2007**, *101*, 997–1004.
(44) Su, Q.; Klinman, J. P. *Biochemistry* **1998**, *37*, 12513–12525.
(45) Marcus, R. A.; Sutin, N. *Biochim. Biophys. Acta* **1985**, *811*, 265–322.
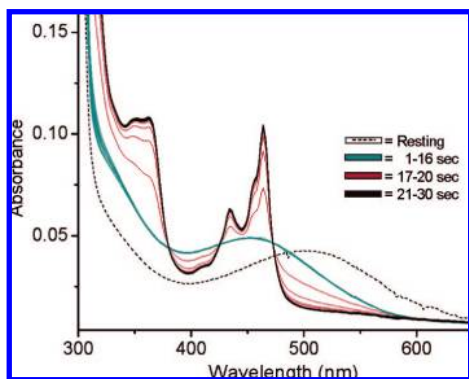
Figure 7. Steady-state accumulation of the product Schiff-base at pH 7.2, $\mu = 0.5$ M and 20 °C.

tion parameters are $\Delta H^{\ddagger} = 11.4 \pm 1.0$ kcal mol^{-1} and $\Delta S^{\ddagger} = 19 \pm 3$ e.u. The observed *positive activation entropy* is inconsistent with a simple bimolecular reaction of O_2, corroborating the proposal, to explain the pH-dependent redox titration and pH-independent kinetics, that $k_{cat}/K_M(O_2)$ reflects a multistep mechanism beginning with reversible binding of O_2.

F. Steady-State Intermediates. Reactions in the presence of saturating O_2 and amine were monitored spectrophotometrically to determine which intermediates accumulate in the steady-state. Experiments were first performed with benzylamine which exhibits $k_{cat} = 0.75$ s^{-1}, K_M(benzylamine) $= 322 \pm 67$ μM and $K_M(O_2) \sim 370$ nM. The $K_M(O_2)$, although too low to be measurable using an O_2 electrode, was calculated from the $k_{cat}/K_M(O_2) = (2.1 \pm 0.2) \times 10^6$ M^{-1}s^{-1} (per monomer) determined with putrescine at 22 °C and pH 7.2 ($\mu = 0.1$ M). Due to the slow turnover rate, the approach to steady-state could easily be monitored with this substrate using a conventional UV−vis spectrophotometer at 20 °C (Figure 7).

The data in Figure 7 were obtained by introducing the enzyme (8.5 μM PSAO, 17 μM TPQ$_{ox}$) into an air saturated solution (284 μM O_2) containing 3.85 mM benzylamine. Upon mixing, the TPQ$_{ox}$ rapidly converts to a species with a broad absorbance centered at 460 nm; this species is assigned as the product Schiff-base on the basis of previous stopped-flow kinetic studies.[46] The absorbance is unchanged as the enzyme continues to turn over (1−16 s) at saturating levels of both substrates. Notably, there is no evidence of TPQ$_{sq}$ accumulation in the steady-state mixture, indicating no contribution from an ET step. The TPQ$_{sq}$ eventually appears (17−30 s) approaching its expected concentration of ∼14 μM as the O_2 is depleted below $K_M(O_2)$.

The observation of the steady-state is more challenging with putrescine because of the elevated kinetic parameters. Values (per monomer) at 22 °C are as follows: $k_{cat} = 91.5 \pm 4.8$ s^{-1}, K_M(putrescine) $= 140 \pm 10$ μM, $K_M(O_2) = 44.6 \pm 4.2$ μM. Experiments required the use of a stopped-flow spectrophotometer for rapid mixing and observation of the reaction solution. The results obtained upon mixing an O_2-saturated solution of PSAO (20 μM, 40 μM TPQ$_{ox}$) with an O_2-saturated solution of putrescine (10 mM) at pH 7.2 and 24 °C are shown in Figure 8. The final concentrations of enzyme and putrescine in the observation cell are one-half of those quoted above, while the O_2 concentration is maintained at ∼1 mM.

Monitoring optical changes between 352−577 nm over 1 s indicated the steady-state was attained in the time of mixing and lasted for ∼250 ms. Between 250 and 320 ms a rapid change gave rise to the spectrum characteristic of the reduced enzyme (10 μM PSAO) containing ∼80% E(Cu^I, TPQ$_{sq}$). Global analysis was used to obtain the initial, steady-state mixture (red) and final, E$_{red}$ (blue) spectra (Figure 8c). In the initial spectrum, the sloping absorbance with $\lambda_{max} = 340$ nm is consistent with the substrate Schiff base[47] while the absorbance at 500 nm indicates the presence of E$_{ox}$ or E$_{im}$. The λ_{max} at 340 nm has also been associated with iminoquinone, TPQ$_{im}$,[48] which would buildup if hydrolysis to form NH$_3$ were rate-limiting. In view of the substrate deuterium KIE and the significant solvent isotope effect of 1.7 ± 0.1 upon k_{cat} at pH 7.2, up to 65% of this steady-state parameter may be limited by NH$_3$ loss with the remaining contribution from C−H deprotonation resulting in accumulation of the optically indistinguishable substrate Schiff-base.

IV. Discussion

Distinguishing inner-sphere from outer-sphere electron transfer (ET) reactions of oxygen is a fundamental problem in biological and inorganic chemistry.[5a,8] The ET mechanisms relate to the origins of catalytic O_2 reduction rates as well as the strategies used by enzymes to avoid oxidative damage by reactive oxygen species.[49] The role of the copper ion during catalysis by copper amine oxidases is a prime example.[19,25,36] Inner-sphere electron transfer, where O_2 binds directly to the Cu^I, was originally assumed based on the observation that a significant fraction of the reduced enzyme existed in the E(Cu^I, TPQ$_{sq}$) state.[13,17,50] Though the expected [Cu$^{II}(\eta^1$-O_2^{-1})]$^+$ intermediate has eluded spectroscopic detection, another species assigned as a Cu$^{II}(\eta^2$-O_2^{-II}) presumably with the accompanying TPQ$_{im}$ has been observed by cryogenic X-ray crystallography studies of the *E. coli* amine oxidase.[14] In the absence of correlations to the enzyme kinetics, it is unclear if and how this intermediate may be involved in catalysis.

Numerous studies undertaken with the yeast enzyme HPAO have been interpreted in the context of an outer-sphere ET mechanism, where the electron transfers from E(Cu^{II},TPQ$_{red}$) to O_2 prebound in a hydrophobic protein pocket.[36,42,44,48,51] The binding step is evidenced by saturation behavior in the O_2-dependent kinetics of the single turnover reaction.[48] The most compelling support for outer-sphere ET comes from the observation that cobalt(II)-reconstituted HPAO catalyzes turnover at rates that approach those of the wild-type enzyme, although $k_{cat}/K_M(O_2)$ is significantly depressed. It has further been argued that the reconstituted HPAO exists exclusively in the Co^{II} state during catalysis.[51] This observation is somewhat surprising in light of the spontaneous nature of reactions between amine-bound Co^{II} and O_2 which form Co^{III} in aqueous solution.[52] Presumably, the protein environment dramatically alters the Co$^{III/II}$ redox potential and, thus, the reactivity of Co^{II} toward

(46) (a) Hartmann, C.; Brzovic, P.; Klinman, J. P. *Biochemistry* **1993**, *32*, 2234–2241. (b) Hartmann, C.; Dooley, D. M. *Methods Enzymol.* **1995**, *258*, 69–90.
(47) Mure, M.; Klinman, J. P. *J. Am. Chem. Soc.* **1995**, *117*, 8707–8718.
(48) Takahashi, K.; Klinman, J. P. *Biochemistry* **2006**, *45*, 4683–4694.
(49) (a) Smirnov, V. V.; Roth, J. P. *J. Am. Chem. Soc.* **2006**, *128*, 16424–16425. (b) Smirnov, V. V.; Roth, J. P. *J. Am. Chem. Soc.* **2006**, *128*, 3683–3695.
(50) Bellelli, A.; Agro, A. F.; Floris, G.; Brunori, M. *J. Biol. Chem.* **1991**, *266*, 20654–20657. Medda, R.; Padiglia, A.; Bellelli, A.; Sarti, P.; Santanche, S.; Finazzi-Agro, A.; Floris, G. *Biochem. J.* **1998**, *332*, 431–437.
(51) Mills, S. A.; Klinman, J. P. *J. Am. Chem. Soc.* **2000**, *122*, 9897–9904.
(52) Cotton, F. A.; Wilkinson, G. *Advanced Inorganic Chemistry*, 5th ed.; Wiley & Sons: New York, 1988; pp 732−733, 735−738.
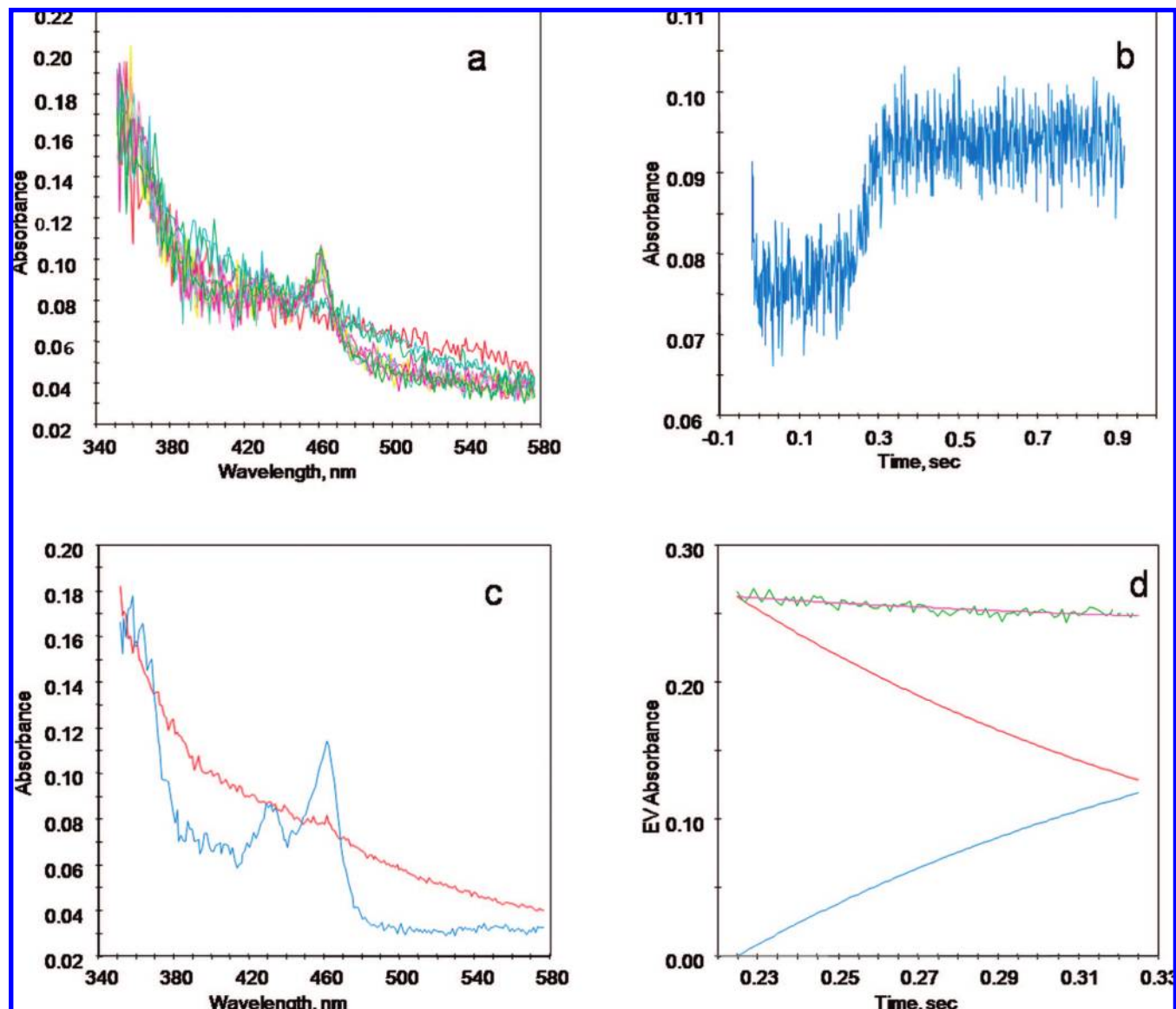
Figure 8. The approach to steady-state in the reaction of PSAO (10 μM) with O_2 (1.0 mM) and putrescine (5 mM) at pH 7.2, $\mu = 0.1$ M and 24 °C. (a) Overlay of spectra collected over 1 s. (b) The absorbance change at 462 nm. (c) The initial and final calculated spectra (see text for details). (d) The changes in concentration corresponding to the initial and final spectra in (c).

O_2. Although an [18]O KIE has been reported for Co-HPAO, the large error in the measurement precludes its interpretation.[42]

Stopped-flow analysis of the single-turnover reaction in wild-type HPAO points toward the first electron transfer in the oxidative half-reaction as contributing roughly 30% to k_{cat}.[48] This is in marked contrast to the results presented here for PSAO, which demonstrate that k_{cat} and $k_{cat}/K_M(O_2)$ do not share a common step. Although there is no spectral evidence, rapid pre-equilibrium to form a high energy E(CuO_2, TPQ_{sq}) intermediate cannot be rigorously excluded based on the single-turnover kinetics. Spectroscopic observation of such copper superoxide intermediates is often difficult due to the unfavorable $\Delta S°$ associated with O_2-coordination as well as their unpredictable magnetic properties.[21] Kinetic methods, such as the oxygen isotope fractionation described here, are therefore needed to detect such species and to assess their involvement in catalysis.[5,19,20,49]

A critical issue which has not been understood in studies of HPAO and bovine serum amine oxidase (BSAO) concerns the

magnitude of the competitive [18]O KIE.[28a] The observations of small [18]O KIEs of ~1.01 are difficult to reconcile with the much larger [18]O KIEs of 1.025−1.030 expected for outer-sphere ET.[19,28a,36,53] In earlier studies,[42,44] an electrostatic interaction between Cu[II] and the incipient O_2•[−] was proposed to cause diminution of the [18]O KIE. For this to be true, the transition state must experience a change in force field which increases the net isotope shift of vibrational frequencies, $\Sigma(^{16,16}\nu - {}^{16,18}\nu)$, relative to the reactant O_2. This explanation presumes a bonding interaction in the transition state and, in turn, contradicts the formal definition of outer-sphere ET.[8] More recently, attention has turned to the possibility that kinetic complexity is responsible for the smaller than expected [18]O KIEs in HPAO and BSAO.[19,36] In this study, we present evidence to the contrary,

(53) Roth, J. P.; Wincek, R.; Nodet, G.; Edmondson, D. E.; McIntire, W. S.; Klinman, J. P. *J. Am. Chem. Soc.* **2004**, *126*, 15120–15131.
(54) Shepard, E. M.; Dooley, D. M. *J. Biol. Inorg. Chem.* **2006**, *11*, 1039–1048.

that ^{18}O KIEs of ~ 1.01 are actually expected upon pre-equilibrium binding of O_2 to Cu^I.

A. Internal Redox Equilibrium in PSAO. In PSAO, the internal redox equilibrium occurs rapidly at physiological pH generating $\sim 80\%$ of the enzyme in the $E(Cu^I, TPQ_{sq})$ state on a time scale compatible with this species' involvement in enzyme catalysis. A similar amount of $E(Cu^I, TPQ_{sq})$ ($\sim 70\%$) is observed in the amine oxidase from lentil seedling (LSAO).[24,50] In contrast, the $E(Cu^{II}, TPQ_{red})$ state dominates, making up >80% of the total reduced enzyme at physiological pH, in HPAO[36] and BSAO.[44] Roughly 50/50 partitioning occurs in the bacterial enzyme from *Arthrobacter globiformis*[54] (AGAO). Clearly, there are differences in the protein active site structures which either promote or inhibit proton-coupled electron transfer and, hence, the equilibration of $E(Cu^{II}, TPQ_{red})$ and $E(Cu^I, TPQ_{sq})$ (Figure 2). The redox potential of the copper ion is likely to be a key factor as it is easily tuned by the protonation state of a bound water molecule.

The weak pH dependence of K_{int} in PSAO possibly reflects stabilization of $Cu^{II}-OH_2$ over the less oxidizing $Cu^{II}-OH$. The slope of the log K_{int} versus pH plot of 0.27 is, however, inconsistent with a simple protonation/deprotonation event. Instead the effect of peripheral residues on either the $E^{\circ\prime}$ or pK_a of $Cu^{II}-OH_2$ is implied. More importantly, from pH 6-10 the concentration of $E(Cu^I, TPQ_{sq})$ varies by a factor of 3 while $k_{cat}/K_M(O_2)$ remains unchanged. A minimal change of a factor of 2.4 would be expected if O_2 were to bind to E_{red} in the rate-determining step.[55] At very low pH, the divergence is magnified by a further increase in $E(Cu^I, TPQ_{sq})$ concentration at the same time $k_{cat}/K_M(O_2)$ decreases by a factor of ~ 2. The lack of correlation between the position of the internal redox equilibrium and the steady-state rate constant is most readily attributed to a multistep mechanism with the rate-determining step occurring only after the reversible binding of O_2.

The electrostatic field which determines K_{int} was expected to be influenced by an active site lysine (Lys296), a residue that is conserved among the plant enzymes.[15] Recent crystallographic studies under high pressures of xenon have suggested the possibility that the Lys is involved in a conformationally gated redox process, where TPQ_{sq} is generated upon oxidative deamination of the side-chain.[56,57] In this study, no significant role for Lys296 in catalyzing the oxidative half-reaction is evident; the $k_{cat}/K_M(O_2)$ in PSAO falls within an order of magnitude of the rate constants determined for HPAO,[42] BSAO,[44] and AGAO,[25] all of which lack the active site Lys.

B. Interpretation of the Steady-State Kinetics. 1. Intermediates during Enzyme Turnover. Spectrophotometrically examining the TPQ-derived species that accumulate in the steady-state affirmed the absence of a common irreversible step in $k_{cat}/K_M(O_2)$ and k_{cat}. Analysis of benzylamine oxidation revealed a small contribution from C-H deprotonation based on the deuterium substrate KIEs[58] and large accumulation of the product Schiff-base at 460 nm, consistent with the release of benzaldehyde limiting k_{cat}. The aldehyde must be released prior to the internal proton-coupled electron transfer, which is needed

to prime the enzyme for reaction with O_2 in the proposed inner-sphere mechanism. Importantly, the prominent absorbance features due to the TPQ_{sq} are absent, indicating that neither the first nor second ET step in the oxidative half-reaction contributes to k_{cat} with benzylamine.

The steps which control k_{cat} for putrescine oxidation are different from benzylamine, as expected due to the 10^2 fold increase in rate constant. Examination of $^Dk_{cat}$ and $^Dk_{cat}/K_M$ at varying pH and temperature indicates a significant contribution from C-H oxidation. The accumulation of the enzyme bound substrate Schiff-base complex, $E_{ox}S$, at 340 nm in the UV-vis spectrum is, therefore, expected. The optical spectrum of the steady-state reaction mixture obtained from global analysis of the stopped-flow data within the first 250 ms bears out this expectation. In addition, the optical density around 500 nm suggests that the spectrum contains some E_{ox} or E_{im} consistent with a contribution from NH_3 dissociation from the TPQ_{im} in the rate-determining step. Again, the spectral features due to TPQ_{sq} are absent, indicating no rate limitation from ET steps in the oxidative half-reaction.

2. Oxidative Half-Reaction. a. Activation Parameters. The kinetic parameter $k_{cat}/K_M(O_2)$ does not share a common step with k_{cat} yet the temperature dependences are similar. The activation parameters in the adiabatic limit[45] for $k_{cat}/K_M(O_2)$ are as follows: $\Delta H^{\ddagger} = 11.4 \pm 1.0$ kcal mol^{-1} and $\Delta S^{\ddagger} = 19 \pm 3$ e.u. The positive entropy of activation argues against a simple bimolecular reaction of E_{red} and O_2. This conclusion echoes that drawn on the basis of the pH dependence of K_{int} and its lack of correlation to $k_{cat}/K_M(O_2)$. The results implicate a multistep process, where ET follows the entropically favored prebinding of O_2.

A common explanation for positive activation entropy in enzymes is the release of structured water from the protein active site.[59] Crystallographic studies reveal two water molecules bound to the Cu^{II} in the E_{ox} state of the copper amine oxidases (Figure 1).[15,16] Release of water is expected upon reduction of Cu^{II} to Cu^I; this reaction is suggested by XAS studies of dithionite-reduced PSAO which revealed a three-coordinate Cu^I center.[60] The dissociation of water upon reduction of Cu^{II} might be a general strategy used by copper-containing proteins to bind O_2 with moderate affinity. The PSAO reaction clearly proceeds with more favorable entropy than related small molecule models. In particular, studies of synthetic copper or cobalt compounds which bind O_2 in an end-on manner are generally characterized by large negative entropy terms.[21,61] Such behavior has also been proposed in O_2-carrier proteins like myoglobin, where O_2 association with the metal center is significantly more favorable than in solution.[62]

(55) The factor of 2.4 is estimated by assuming that O_2 reacts preferentially with the $E(Cu^I, TPQ_{sq})$ and considering the total enzyme concentration given by: $[E]_T = [E(Cu^I, TPQ_{sq})] + [E(Cu^{II}, TPQ_{red})] = [E(Cu^I, TPQ_{sq})](K_{int} + 1/K_{int})$ where $K_{int} = 5.9$ at pH 6 and 0.48 at pH 10.
(56) Duff, A. P.; Trambaiolo, D. M.; Cohen, A. E.; Ellis, P. J.; Juda, G. A.; Shepard, E. M.; Langley, D. B.; Dooley, D. M.; Freeman, H. C.; Guss, J. M. *J. Mol. Biol.* **2004**, *344*, 599–607.
(57) Mura, A.; Anedda, R.; Pintus, F.; Casu, M.; Padiglia, A.; Floris, G.; Medda, R. *FEBS J.* **2007**, *274*, 2585–2595.

(58) Similar intrinsic isotope effects upon C-H, containing small contributions from deuterium in the secondary position, have been reported for BSAO, Farnum, M.; Palcic, M.; Klinman, J. P. *Biochemistry* **1986**, *25*, 1898–1904. Grant, K. L.; Klinman, J. P. *Biochemistry* **1989**, *28*, 6597–6605. Significantly larger kinetic isotope effects have been reported in AGAO, Murakawa, T.; Okajima, T.; Kuroda, S.; Nakamoto, T.; Taki, M.; Yamamoto, Y.; Hayashi, H.; Tanizawa, K. *Biochem. Biophys. Res. Commun.* **2006**, *342*, 414–423.
(59) Loftfield, R. B.; Eigner, E. A.; Pastuszyn, A.; Lovgren, T. N.; Jakubowski, H. *Proc. Nat. Acad. Sci. USA* **1980**, *77*, 3374–3378.
(60) Dooley, D. M.; Scott, R. A.; Knowles, P. F.; Colangelo, C. M.; McGuirl, M. A.; Brown, D. E. *J. Am. Chem. Soc.* **1998**, *120*, 2599–2605.
(61) Lanci, M. P.; Roth, J. P. *J. Am. Chem. Soc.* **2006**, *128*, 16006–16007.
(62) (a) Wang, M-Y. R.; Hoffman, B. M.; Shire, S. J.; Gurd, F. R. N. *J. Am. Chem. Soc.* **1979**, *101*, 7394–7397. (b) Walker, F. A. *J. Am. Chem. Soc.* **1973**, *95*, 1154–1159.
(63) Goto, Y.; Klinman, J. P. *Biochemistry* **2002**, *41*, 13637–13643.

An alternative explanation for the positive $\Delta S^{\ddagger}$ in PSAO is that water release occurs upon binding of O_2 in an off-copper, hydrophobic pocket of the protein. In HPAO and BSAO, the partitioning of O_2 into a nonmetal site forms the basis of the argument in favor of rate-determining outer-sphere ET,[36,42,44] explaining why the wild type and cobalt enzymes exhibit similar values of k_{cat}. Though this phenomenon of O_2 "binding" in hydrophobic protein pockets is not well-understood, it derives support from mutagenesis studies of HPAO[63] and more broadly from NMR[64] and X-ray crystallography under high pressures of xenon.[10,56,57] Additional support comes from studies which reveal the collection of CO at nonmetal sites in heme proteins responsible for gas transport.[65] The affinity of these sites for a diatomic gas molecule has been difficult to address, however.

b. Viscosity Studies. In earlier studies of BSAO[44] and HPAO,[42] viscosity effects were used to assess the extent to which diffusion of O_2 contributes to $k_{cat}/K_M(O_2)$. Very high viscosogen concentrations are required in these experiments due to the small size of O_2 and resulting deviations from Stokes−Einstein behavior.[27,66] In the present study, solutions of high relative viscosity were employed yet none revealed an effect that could be construed in terms of a diffusion-controlled reaction.

The absence of a viscosity effect upon $k_{cat}/K_M(O_2)$ does not, in itself, preclude the binding of O_2 to the enzyme in the rate-determining step. For small molecules in solution, these reactions are thermally activated not encounter-controlled. Typically, $\Delta G^{\ddagger} \gg 5$ kcal mol^{-1} is observed as a result of significant $\Delta H^{\ddagger}$ and $-T\Delta S^{\ddagger}$ contributions. In support of the view that O_2 coordination requires overcoming a significant activation barrier, studies of competitive ^{18}O KIEs have revealed variations within the upper limit approximated by the ^{18}O EIE and correlations to the size of $\Delta G^{\ddagger}$.[67] This behavior is expected to be the same in metalloenzymes, allowing changes in transition state structure upon binding of O_2 to be interpreted through comparison of the ^{18}O KIEs to the ^{18}O EIEs for the O_2-adducts.

c. Oxygen Kinetic Isotope Effects. Some of the earliest isotope fractionation measurements were performed on copper amine oxidases.[28a] The ^{18}O KIE of 1.0097 ± 0.0010 determined for BSAO spanned a range of pH values and was proposed, on the basis of the absence of a viscosity effect and of significant TPQ_{sq} accumulation in the steady-state, to reflect outer-sphere ET.[44] The present work challenges the conclusions drawn for BSAO largely because of the ^{18}O KIE.

Recent studies have addressed the isotope effects upon outer-sphere ET to O_2. The major finding, both experimentally and computationally, is that the ^{18}O KIEs range from $1.025-1.030$ when the reaction is close to thermoneutral.[19,28a,49a,53] The ^{18}O KIEs are predicted to drop below 1.025 when ΔG° becomes very favorable. To account for the low values seen for BSAO within the context of an outer-sphere ET mechanism, $\Delta G^{\circ} = -10$ kcal mol^{-1} would be required. Yet, thermodynamic

considerations detailed below indicate that ΔG° for ET from TPQ_{red} to O_2 should be unfavorable.

More recently, kinetic complexity in the O_2 reduction step has surfaced as a possible explanation of the small ^{18}O KIEs seen for HPAO (1.0101 ± 0.0018) and possibly BSAO.[19] An important result is provided by site-directed mutagenesis studies of HPAO in which an even smaller ^{18}O KIE $= 1.0074 \pm 0.0008$ was determined for the D630N mutant.[56] Interestingly, D630N HPAO forms significantly more $E(Cu^I, TPQ_{sq})$ (36%) than the wild-type enzyme (15%) and exhibits a 4-fold increased $k_{cat}/K_M(O_2)$. Klinman and co-workers have maintained that the enzyme reacts by outer-sphere ET citing kinetic complexity as a possible origin of the diminished ^{18}O KIE.[36] Such complexity may arise from (i) a partially rate-limiting step prior to the first ET, such as O_2 "binding" to a nonmetal site or (ii) a partially rate limiting step downstream of the first ET, such as the binding of the $O_2{\bullet}^-$ to Cu^{II}.

The ^{18}O KIEs determined in this study for PSAO are only slightly larger than those seen in HPAO and BSAO yet temperature and pH studies provide no indication of kinetic complexity. The ^{18}O KIE $= 1.0136 \pm 0.0014$ is unchanged from $5-47$ °C. That changing the reaction temperature and pH results in fortuitous cancelation of factors which cause the ^{18}O KIE to be invariant seems very unlikely. Rather the ^{18}O KIE determined for PSAO appears to reflect the intrinsic value, which we show in the following section using DFT methods, to be fully consistent with pre-equilibrium binding of O_2 to form $[Cu^{II}(\eta^1-O_2^{-1})]^+$. Rate-determining ET from the TPQ_{sq} follows as indicated by analysis of the limiting ^{18}O equilibrium isotope effects (EIEs) and the lack of evidence for proton transfer from the kinetic profiles in H_2O and D_2O.

d. Density Functional Calculations. The ^{18}O EIEs calculated for potential intermediates in PSAO are presented in Table 1. The structures are arranged roughly in order of decreasing O−O stretching frequency and increasing O−O bond length. All calculations were performed using the full sets of vibrational frequencies for the $^{16}O-^{16}O$ and $^{16}O-^{18}O$ isotopologues, as we have previously described.[21,34] Modeling the temperature dependence demonstrated that, in most cases, the magnitude of the calculated ^{18}O EIE at 22 °C is indistinguishable from the maximum.[34] The influence of dielectric constant, which is exceedingly difficult to model in an enzyme active site, was neglected since we previously observed that application of a polarized solvent continuum model can alter the stretching frequencies but only slightly affects the ^{18}O EIE.[21]

The underlying assumption in using ^{18}O equilibrium isotope effects (^{18}O EIEs) as limiting values for ^{18}O KIEs is that the change in bonding, or O_2 activation, in the transition state is more advanced than in the intermediate which precedes its formation. The trends seen in the DFT calculations suggest that this should be the case in instances where the contribution from the reaction coordinate frequency can be neglected.[28a,67]

In order to have confidence in our computational modeling, we examined 16 different structures manipulating the various factors which could impact the ^{18}O EIE. These factors include the addition of hydrogen-bonding interactions with water molecules, substituting the more electron-rich methylimidazole for imidazole and constraining one methylimidazole ligand to interact through the more sterically encumbered δ-nitrogen, as seen in the published crystal structure of PSAO.[15] The variables appeared to have little impact on the calculated ^{18}O EIEs, the primary determinant being the O–O and Cu–O bonds. This is not to say that the localized copper−oxygen modes could be

(64) (a) Tilton, R. F., Jr.; Singh, U. C.; Weiner, S. J.; Connolly, M. L.; Kuntz, I. D., Jr.; Kollman, P. A.; Max, N.; Case, D. A. *J. Mol. Biol.* **1986**, *192*, 443–456. (b) Tilton, R. F., Jr.; Kuntz, I. D., Jr. *Biochemistry* **1982**, *21*, 6850–6857. (c) Ewing, G. J.; Maestas, S. *J. Phys. Chem.* **1970**, *74*, 2341–2344.

(65) Steinbach, P. J.; et al. *Biochemistry* **1991**, *30*, 3988–4001.

(66) Roth, J. P.; Klinman, J. P. *Proc. Natl. Acad. Sci. USA.* **2002**, *100*, 62–67.

(67) Lanci, M. P.; Brinkley, D. W.; Stone, K. L.; Smirnov, V. V.; Roth, J. P. *Angew. Chem., Int. Ed.* **2005**, *44*, 7273–7276.

(68) Cramer, C. J.; Tolman, W. B.; Theopold, K. H.; Rheingold, A. L. *Proc. Natl. Acad. Sci. USA.* **2003**, *100*, 3635–3640.

Table 1. Energy Minimized Structures Used to Compute Equilibrium Oxygen Isotope Effects (^{18}O EIEs)

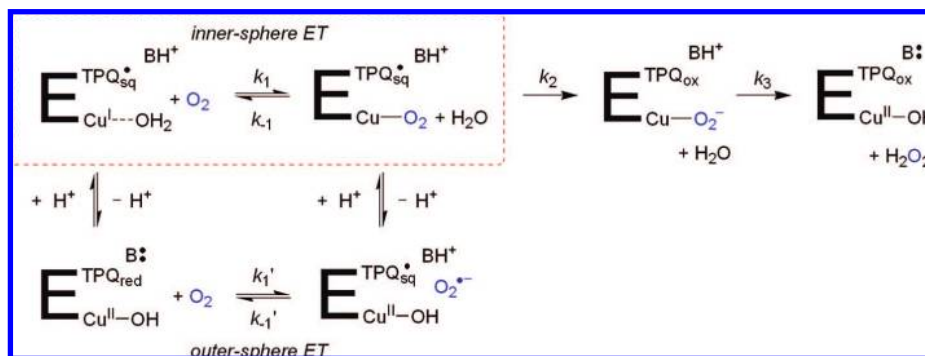|	Structure[a]	$\nu(^{16}O-^{16}O)$ (cm^{-1})	d(O–O) (Å)	^{18}O EIE$_{max}$ (O$_2\rightarrow$ product)[f]	^{18}O EIE (22 °C)
1	O$_2$	1550	1.221	—	—
2	[Cu^{II}(η^1–O$_2$$^{-1}$)(Im)$_3$]$^{+}$ [b]	1342	1.257	1.0108 (-70°C)	1.0092
3	[Cu^{II}(η^1–O$_2$$^{-1}$)(OH$_2$)(Im)$_3$]$^{+}$ [b]	1249	1.285	1.0095 (24 °C)	1.0095
4	[Cu^{II}(η^1–O$_2$$^{-1}$)(MeIm)$_3$]$^{+}$ [b]	1339,1343	1.250	1.0104 (-70°C)	1.0092
5	[Cu^{II}(η^1–O$_2$$^{-1}$)(MeIm)$_2$($\delta$-MeIm)]$^{+}$ [c]	1341, 1344	1.256	1.0107 (-79 °C)	1.0094
6	Cu^{II}(η^1– O$_2$$^{-II}$)(Im)$_3$ [d]	1124.8	1.350	1.0308(-144°C)	1.0214
7	Cu^{II}(η^1– O$_2$$^{-II}$)(Im)$_3$ • H$_2$O [d,e]	1088, 1107	1.355	1.0196 (-62 °C)	1.0178
8	Cu^{II}(η^1– O$_2$$^{-II}$)(MeIm)$_3$ [d]	1114	1.355	1.0275 (-125 °C)	1.0209
9	[Cu^{II}(η^1–O$_2$$^{-II}$)(MeIm)$_2$($\delta$-MeIm)] [c,d]	1069	1.366	1.0340 (-139 °C)	1.0240
10	O$_2$$^{\bullet-}$	1097	1.363	$\rightarrow \infty$ (-273 °C) [g]	1.0310
11	Cu^{II}(η^2– O$_2$$^{-II}$)(Im)$_3$ [d]	997	1.403	1.0631(-209°C)	1.0313
12	Cu^{II}(η^2– O$_2$$^{-II}$)(Im)$_3$ • H$_2$O [d,e]	956	1.427	1.0359(-136 °C)	1.0272
13	Cu^{II}(η^2– O$_2$$^{-II}$)(MeIm)$_3$ [d]	988	1.400	1.0643(-199°C)	1.0313
14	[Cu^{II}(η^2–O$_2$$^{-II}$)(MeIm)$_2$($\delta$-MeIm)] [c,d]	973, 978	1.416	1.0559 (-181 °C)	1.0311
15	[Cu^{II}(η^1–O$_2$$^{-II}$H)(Im)$_3$]$^{+}$ [d]	899	1.428	1.0145 (-29 °C)	1.0139
16	[Cu^{II}(η^1–O$_2$$^{-II}$H)(OH$_2$)(Im)$_3$]$^{+}$ [d]	886, 852	1.447	1.0114 (23°C)	1.0114
17	[Cu^{II}(η^1–O$_2$$^{-II}$H)(MeIm)$_3$]$^{+}$ [d]	911	1.421	1.0118 (-1 °C)	1.0117
18	[Cu^{II}(η^1–O$_2$$^{-II}$H)(MeIm)$_2$($\delta$-MeIm)]$^{+}$ [c,d]	900	1.424	1.0127 (-8 °C)	1.0125

[a] Formal oxidation states are assumed. Entries 6−9 can be reformulated as Cu^I(η^1-O$_2$$^{-1}$) based on the increased copper character in the SOMO. Details are provided in the supporting information. [b] A triplet ground state is assumed.[21] [c] δ-MeIm denotes that the methylimidazole ligand was constrained to coordinate through the δ-nitrogen adjacent to the methyl group. [d] Doublet ground state. [e] The water molecule is dissociated from the copper yet hydrogen bonded to the terminal oxygen of the peroxide ligand. [f] The approximate temperature at which the ^{18}O EIE passes through a maximum is given in parentheses. [g] The EIE approaches infinity as the temperature approaches absolute 0.

used in isolation to give accurate assessment of the ^{18}O EIE. To the contrary, we have found that there is a significant contribution to the ^{18}O EIE from low frequency ligand modes which couple to the ν_{O-O}, ν_{Cu-O}, and δ_{Cu-O-O} vibrations.[34]

e. Interpretation of the Oxygen Kinetic Isotope Effect. The ^{18}O KIEs determined for copper amine oxidases from different sources range from 1.0075 to 1.0136. The effects are close to the limits predicted for the formation of a superoxide, [Cu^{II}(η^1-O$_2$$^{-1}$)]$^{+}$, intermediate. Entries 2−5 in Table 1 indicate a narrow range of values from 1.0092 to 1.0095 corresponding to this structure. When the ^{18}O KIE significantly exceeds 1.0095, as in PSAO, a pre-equilibrium binding of O$_2$ to reversibly form

Scheme 1. Kinetic Mechanism for the Oxidative Half-Reaction of PSAO

the $[Cu^{II}(\eta^1\text{-}O_2{}^{-1})]^+$ is indicated. In earlier work,[67] we showed that in cases of irreversible O_2 binding the ^{18}O KIEs are depressed, approaching the ^{18}O EIEs only when kinetic barriers are very high $\Delta G^{\ddagger} \geq 15$ kcal mol^{-1}. Rate-determining O_2-binding may occur in the D630N mutant of HPAO, where the ^{18}O KIE is less than the calculated ^{18}O EIE for the formation of the $[Cu^{II}(\eta^1\text{-}O_2{}^{-1})]^+$ intermediate.

A number of results point toward a multistep process involving reversible O_2 binding in PSAO. These results include the absence of a viscosity effect, the positive entropy of activation determined in temperature studies, the lack of correlation between the position of K_{int} and $k_{cat}/K_M(O_2)$ as well as the favorable comparison of the ^{18}O KIE to the calculated ^{18}O EIE for the $[Cu^{II}(\eta^1\text{-}O_2{}^{-1})]^+$ structure.

DFT calculations on the minimum energy end-on peroxide, $Cu^{II}(\eta^1\text{-}O_2{}^{-II})$, and side-on peroxide, $Cu^{II}(\eta^2\text{-}O_2{}^{-II})$, structures indicate large ^{18}O EIEs. Values of 1.017–1.024 and 1.027–1.031, respectively, mark the expected limits for the observed ^{18}O KIE. The variation within the calculated ^{18}O EIEs for the end-on structure reflects the influence of hydrogen bonding to a water molecule (cf. entry 7 versus entries 6, 8, and 9). The smaller range seen for the side-on structure (entries 11–14) reflects the insensitivity of the isotope effect to the steric and electronic changes which occur upon replacing imidazole with methylimidazole and forcing one ligand to coordinate through the δ-nitrogen.

Peroxide structures are potential products of the rate-limiting step in PSAO, i.e., the ^{18}O KIE reflects all steps which contribute to $k_{cat}/K_M(O_2)$ beginning with O_2 encounter and leading up to the first irreversible step. The end-on structure is favored over the side-on structure because the $Cu^{II}(\eta^2\text{-}O_2{}^{-II})$ represents a local minimum with its energy 2.3 to 4.8 kcal mol^{-1} greater than the $Cu^{II}(\eta^1\text{-}O_2{}^{-II})$. In order to keep both O nuclei coordinated to Cu^{II} in the side-on structure it was necessary to rotate the imidazole rings to a conformation where the higher energy geometry was accessible. It is interesting that coordination of dioxygen as a side-on peroxide ligand has been reported in a crystallographic study of *E. coli* amine oxidase,[14] though it is unclear whether such an intermediate would form during catalysis in solution.

In the $Cu^{II}(\eta^1\text{-}O_2{}^{-II})$ proposed as the product of the rate-determining ET step in PSAO, the added electron appears significantly delocalized into the copper d_{xy} orbital. Inspection of the singly occupied molecular orbital,[34] together with the calculated ν_{O-O} and O–O bond distances in Table 1, indicates a continuum bonding description[68] where there is significant $Cu^I(\eta^1\text{-}O_2{}^{-1})$ character. This scenario changes when a proton is transferred to the terminal oxygen affording $[Cu^{II}(\eta^1\text{-}$

$O_2{}^{-II}H)]^+$. The absence of a more sizable solvent kinetic isotope effect upon $k_{cat}/K_M(O_2)$ in PSAO argues against the formation of the protonated peroxide species in the first irreversible step. The ^{18}O EIEs calculated for this structure (1.011–1.014, entries 15–18) are mostly too small to be consistent with the observed ^{18}O KIE.

C. Inner-Sphere Mechanism of O_2 Reduction. The proposed O_2 reduction mechanism in PSAO involving reversible O_2 binding to Cu^I followed by ET from the TPQ_{sq} in the first irreversible step is shown in Scheme 1. The supporting evidence includes (i) the lack of correlation between $k_{cat}/K_M(O_2)$ and K_{int}. (ii) the positive $\Delta S^{\ddagger}$ derived from the temperature studies of $k_{cat}/K_M(O_2)$, (iii) the absence of rate-limitation by proton transfer, (iv) the absence of an encounter-controlled reaction of O_2, and (v) the competitive ^{18}O KIE which is ostensibly free of kinetic complexity and lies between that calculated for the $[Cu^{II}(\eta^1\text{-}O_2{}^{-1})]^+$ and $Cu^{II}(\eta^1\text{-}O_2{}^{-II})$. The latter superoxide and peroxide structures are associated with $Cu-O_2$ and $Cu-O_2^-$, respectively, in Scheme 1.

In addition to accounting for the size of ^{18}O KIE observed for copper amine oxidases, the mechanism in Scheme 1 might explain the lack of a correlation between the pH dependences of K_{int} and $k_{cat}/K_M(O_2)$. If O_2 were to act as a "sticky" substrate, then the kinetically determined pK_a values could be shifted outside of the experimental range. To understand this effect, the forward commitment to catalysis must be considered.[40] According to Scheme 1, eq 6 is the rate expression for $k_{cat}/K_M(O_2)$.[40b] Making the simplifying assumption that the rate constants for the initial ET steps are equal ($k_1 = k_1'$), eq 6 reduces to eq 7. Equation 7 contains a term, $C_f = k_2/k_{-1}$ that corresponds to the internal forward commitment factor. The expression can be rewritten in terms of eq 8 from which it is now obvious that when C_f is large, or O_2 is "sticky", the measured pK_a will be elevated from the intrinsic value. This behavior could explain the absence of a titratable residue in the pH profile of $k_{cat}/K_M(O_2)$ in PSAO. The observation of such a residue was anticipated on the basis of pK_a values of ~9 determined for copper(II) bisaquo complexes,[69] which resemble the copper amine oxidase active site, as well as the pK_a of 7.7 assigned to the $Cu^{II}-OH_2$ in HPAO.[42]

$$k_{cat}/K_M(O_2) = \frac{k_2\{k_1 + k_1'(K_a/[H^+])\}}{\{1 + (K_a/[H^+])\}\{k_2 + k_{-1} + (K_a k_1 k_{-1}/k_1'[H^+])\}} \quad (6)$$

$$k_{cat}/K_M(O_2) = \frac{k_2 k_1/k_{-1}}{C_f + 1 + K_a/[H^+]} \quad (7)$$

$$pK_a(\text{intrinsic}) = pK_a(\text{measured}) - \log(1 + C_f) \qquad (8)$$

D. Catalysis of O_2 Reduction. 1. Thermodynamic Considerations. The ability of copper amine oxidases to reduce O_2 to H_2O_2 is ultimately determined by the $2e^-$ redox potential of the reduced enzyme. The rate of the reaction can be understood in terms of the thermodynamics of the rate-determining step according to the tenets of Marcus theory.[45] We have previously shown that this is a useful formalism for understanding catalysis of ET as well as the propensity of an enzyme to react by an inner-sphere or outer-sphere pathway.[49,53,66]

Concentrating first on the feasibility of outer-sphere ET in copper amine oxidase, the thermodynamic driving force, $\Delta G°$, is defined by the one-electron redox potentials of TPQ_{red} and O_2. The $\Delta G°$ can be estimated using a thermodynamic cycle for TPQ_{red} following the method of Bordwell.[70]

As a starting point, solution bond dissociation free energies are related to $E°$ and pK_a values through Scheme 2. The relationship employs a thermodynamic constant $C = 57$ kcal mol^{-1} which reflects the formation and solubilization of the $H\bullet$ in aqueous solution.[71] This type of analysis has been used widely to evaluate the bond dissociation free energies for a wide variety of inorganic and organic compounds, including substituted phenols. For TPQ_{red} the diagonal of the square scheme is determined to be $\Delta G°_{H\bullet} = 18$ kcal mol^{-1} by subtracting C from the O−H bond dissociation free energy (BDE). To be conservative, the TPQ_{red} was assumed to have a BDE $= 75$ kcal mol^{-1}, comparable to that reported for 4-aminophenol.[70]

Following the square scheme, from left to right and then down, $\Delta G°_{H\bullet}$ is adjusted by $\Delta G°_{H+}$ ($= -RT\ln K_a$), reflecting the pK_a of the semiquinone cation radical $TPQ_{sq}H^+$, to obtain the driving-force for ET, $\Delta G°_{e-}$ ($= -nFE°$).[72] Pulse radiolysis studies of the cofactor in solution have indicated a $pK_a \approx 3.4$ for $TPQ_{sq}H^+$.[39] The value is consistent with our observations that the optical spectrum of the TPQ_{sq} in PSAO does not shift or broaden as the pH is lowered from 10 to 5.5. Conservatively taking the $pK_{a\,(1)}$ of the $TPQ_{sq}H^+$ to be <5 makes $E°_{(1)} = 0.48$ V vs NHE a lower limit for the sought after TPQ_{red} one-electron redox potential.

The free energy for outer-sphere ET from reduced PSAO to O_2 can be derived from the difference of $E°(O_2/O_2^-) = -0.16$ V vs NHE and $E°_{(1)}$. In the absence of electrostatic stabilization, the reaction is clearly very unfavorable with $\Delta E° \leq -0.64$ V or $\Delta G° \geq 14.8$ kcal mol^{-1} at 22 °C. Yet $\Delta G^{\ddagger} = 5.8 \pm 1.3$ kcal mol^{-1} is calculated from $k_{cat}/K_M(O_2)$ in PSAO. *That the observed barrier is much lower than the lower limit of the calculated thermodynamic barrier argues strongly that outer-sphere ET from the neutral aminoquinol is not a viable mechanism.* Though electrostatic stabilization of the $O_2^{\bullet-}$ and/or the $TPQ_{sq}^{\bullet+}$ could make the reaction less unfavorable, it is difficult to envisage how such an interaction could reduce $\Delta G°$ by >9 kcal mol^{-1}.

The same analysis can be used to evaluate the possibility of outer-sphere electron transfer from the deprotonated amino-

Scheme 2. Thermodynamic Cycle for Assessing the Driving-Force for TPQ_{red} Oxidation
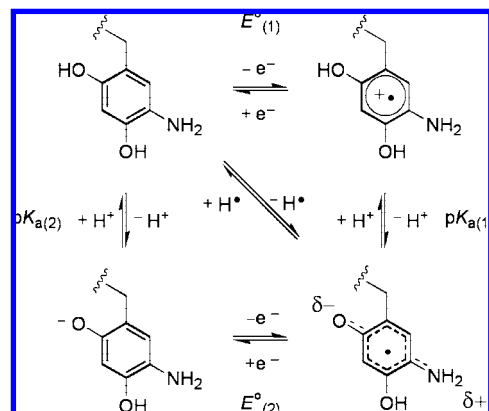
quinol. A pK_a of 9.6 has been estimated for the neutral cofactor based on model studies described in Results section A.[37] Using this value, corresponding to a free energy of 13.15 kcal mol^{-1}, together with the $\Delta G°_{H\bullet} = 18$ kcal mol^{-1}, indicates $\Delta G°_{(2)} = 4.85$ kcal mol^{-1} or $E°_{(2)} = 0.21$ V vs NHE. Solving $E°(O_2/O_2^-) - E°_{(2)} = -0.37$ V vs NHE, i.e., $\Delta G° = 8.5$ kcal mol^{-1}. This thermodynamic barrier is less unfavorable than for the neutral cofactor but still significantly larger than the observed $\Delta G^{\ddagger}$. It is certainly possible that enzyme active sites can alter reaction thermodynamics through strategically placed charged residues; though no evidence to this effect has been reported as yet in the copper amine oxidases. In flavoenzymes where outer-sphere ET to O_2 is catalyzed by lowering of the intrinsic reorganization energy (λ), electrostatic stabilization of -3.5 kcal mol^{-1} has been estimated.[66] Such a stabilization energy in the copper amine oxidases could make $\Delta G°$ approximate $\Delta G^{\ddagger}$, though an additional contribution would still be required to minimize λ and make the kinetic barrier negligible.

In light of the thermodynamics for the resting reduced PSAO, we propose that the presence of Cu^I biases O_2 reduction to proceed by an inner-sphere electron transfer pathway. The $Cu-O_2$ bond has significant covalent as well as ionic character.[18] Using outer-sphere redox potentials and equilibrium constants for forming $Cu-O_2$ adducts, the interaction energy of Cu^{II} and $O_2^{\bullet-}$ has been estimated to exceed 25 kcal mol^{-1}.[8,21] This stabilizing interaction associated with inner-sphere ET upon binding of O_2 to Cu^I is needed to lower $\Delta G°$ to the extent necessary to make $\Delta G^{\ddagger}$ comparable to the observed barrier of 5.8 kcal mol^{-1}.

2. Intrinsic Barrier to O_2 Reduction. Favorable $\Delta G°$, together with preorganized electrostatics of a protein active site, can result in lowering of the barrier to O_2 reduction. Electrostatic catalysis, where the λ associated with outer-sphere ET to O_2 is dramatically reduced relative to its value in solution, has been described in glucose oxidase[66] and may exist in many other flavoproteins[73] as well as quinoproteins.[74] Thus, the question arises as to the role of positively charged residues such as the Lys residue conserved among plant amine oxidases.

In PSAO, Lys296 is positioned such that it can lower the pK_a of the amino group in TPQ_{red} and possibly facilitate the deprotonation of the 2- or 4-hydroxyl group through an electrostatic field effect. The formation of TPQ_{red}^- would be followed by rapid ET to yield the $E(Cu^I, TPQ_{sq})$ state which

(69) Scarpellini, M.; Neves, A.; Hoerner, R.; Bortoluzzi, A. J.; Szpoganics, B.; Zucco, C.; Silva, Rene, A. N.; Drago, V.; Mangrich, A. S.; Ortiz, W. A.; Passos, W. A. C.; De Oliveira, M. C. B.; Terenzi, H. *Inorg. Chem.* **2003**, *42*, 8353–8365.
(70) Bordwell, F. G.; Cheng, J. *J. Am. Chem. Soc.* **1991**, *113*, 1736–1743.
(71) Mayer, J. M. in *Biomimetic Oxidations Catalyzed by Transition Metal Complexes*; Meunier, B., Ed.; Imperial College Press: London, 2000; pp 1−43
(72) The n represents the number of electrons transferred and F is Faraday's constant $= 23.06$ kcal mol^{-1}/V.

(73) Massey, V. *Int. Congr. Ser.* **2002**, *1233*, 3–11.
(74) Klinman, J. P. *J. Biol. Inorg. Chem.* **2001**, *6*, 1–13.

we have shown dominates the reduced PSAO at physiological pH. Yet $k_{cat}/K_M(O_2)$ for PSAO is within an order of magnitude of values reported for HPAO[42] and BSAO[44] indicating that Lys296 does not dramatically influence the $\Delta G^{\ddagger}$ for O_2 reduction. The residue might, however, alter relevant pK_a values which control ET through the kinetically labile copper bound water molecules.

What then causes the rate of copper amine oxidase catalyzed O_2 reduction to exceed those of the analogous uncatalyzed reactions in solution? Several years ago, Merényi and co-workers demonstrated outer-sphere ET from 4-aminophenolate to O_2 that occurs with a rate constant of 7.9 $M^{-1}s^{-1}$.[75] Applying Marcus Theory[45] indicated $\lambda = 37$ kcal mol^{-1} for this reaction. Assuming for a moment that the same outer-sphere ET mechanism is operative in copper amine oxidases, which exhibit 10^5-fold rate acceleration, suggests that λ must be lowered on the enzyme by more than 20 kcal mol^{-1}. Yet, in spite of the extensive mutagenesis studies performed on HPAO,[36,63] none has exposed an amino acid residue which could be considered responsible for this catalytic effect. In one notable active site mutant, D630N HPAO, a rate increase relative to the wild-type enzyme is observed. These results would seem indicative of robustness and plasticity rather than an electrostatically preorganized active site.[66]

The thermodynamic considerations described above suggest another strategy for lowering the barrier to O_2 reduction in copper amine oxidase which simply involves inner-sphere ET. The accessibility of the E(Cu^I, TPQ$_{sq}$) is a critical factor. Most if not all copper amine oxidases[13,17,42,35,36,44,50] produce the E(Cu^I, TPQ$_{sq}$) although studies to test the kinetic competence of the intermediate have only been performed with PSAO[15] and AGAO.[35] A critical test of the inner-sphere mechanism in the other copper amine oxidases would involve determining the intraprotein proton-coupled electron transfer rate constants which contribute to K_{int} (cf. Figure 2). It is not until such experiments are performed that we can generalize the observations described in this work.

Nevertheless, we point out that the formation of a covalently bound $[Cu^{II}(\eta^1\text{-}O_2^{-I})]^+$ intermediate derived from the inner-sphere reaction of Cu^I and O_2 would enhance the rate by making $\Delta G°$ significantly more favorable than it would be otherwise; noting again $\Delta G° > 14.8$ kcal mol^{-1} is estimated for the outer-sphere reaction between E(Cu^{II}, TPQ$_{red}$) and O_2. Another possibility, which cannot be discounted, is that the formation of such an intermediate in HPAO is thermodynamically favored yet kinetically disfavored by a coordination inert copper center. This type of kinetic barrier to O_2 coordination might be imposed through deprotonation of the Cu^I-bound water if such species exists. Further, the presence of Cu^{II}OH might stabilize the anionic aminoquinol with respect to intraprotein ET to the Cu^{II}. We add that in none of the enzymes should the formation of the putative $[Cu^{II}(\eta^1\text{-}O_2^{-I})]^+$ be so far downhill that the intermediate becomes observable using conventional spectroscopy. Rather the second ET from the TPQ$_{sq}$ appears required to form the Cu$^{II}(\eta^1\text{-}O_2^{-II})$ and render O_2 reduction irreversible.

V. Conclusions

These are the first studies to support an inner-sphere electron transfer mechanism during the catalytic reduction of molecular oxygen by copper amine oxidases. Much effort has been devoted

to the study of these enzymes from other sources culminating in proposals of partially rate-determining outer-sphere ET from the fully reduced TPQ cofactor to O_2. The findings from the present work provide the first compelling evidence to the contrary and suggest new experiments for some of the systems which have been previously investigated.

Experimental and computational support has been obtained for O_2 binding reversibly to the reduced pea seedling amine oxidase followed by ET from the TPQ semiquinone cofactor in the rate-determining step. More specifically, the evidence for reversible O_2 binding to Cu^I comes from studies of rates as a function pH as well as temperature and the observation of a competitive ^{18}O KIE, free of kinetic complexity, which falls squarely within the limits expected for an end-on copper superoxide $[Cu^{II}(\eta^1\text{-}O_2^{-I})]^+$ structure and an end-on copper peroxide Cu$^{II}(\eta^1\text{-}O_2^{-II})$ structure. The boundary conditions set by superoxide and peroxide structures were calculated by the full set of vibrational frequencies obtained using a recently established density functional method. Thus, the application of a combined experimental/computational approach provides benchmarks that should be generally useful for identifying kinetically significant metal−oxygen intermediates which are not observable using conventional spectroscopic methods.

In addition to novel mechanistic findings for a plant-derived copper amine oxidase, thermodynamic analyses of the proposed electron transfer reactions have been presented. The results clearly indicate that outer-sphere electron transfer from the neutral reduced cofactor to O_2 is highly unfavorable and incompatible with observed free energy barriers for O_2 reduction. The electron transfer from the deprotonated aminoquinol cofactor, a reaction which had not been considered previously, is also unfavorable but less so. Additional experiments will be required to test the kinetic competence of the Cu^I state in the yeast and bovine serum enzymes. If such a state were accessible, then the analyses presented here would suggest O_2 activation by an inner-sphere electron transfer mechanism. This is the proposed mechanism for pea seedling amine oxidase, where O_2 binds directly to Cu^I in an initial slightly favorable to unfavorable step followed by electron transfer from the TPQ semiquinone to drive the reaction forward. Such inner-sphere ET reactivity may be a strategy exploited by various enzymes, which possess redox active and coordination labile metal centers, to avoid the uncoupled reduction of O_2 and the accumulation of damaging reactive oxygen species during catalysis.

Supporting Information Available: Includes details concerning the methods used to calculate oxygen isotope effects, graphics showing the minimum energy structures and molecular orbitals as well as list of the complete set of computed vibrational frequencies for each structure. This material is available free of charge via the Internet at http://pubs.acs.org.

(75) Merényi, G.; Lind, J.; Jonsson, M. *J. Am. Chem. Soc.* **1993**, *115*, 4945–4946.

JA801378F